

# Optimal Sampling for Kernel Quadrature on Unbounded Domains

Edoardo Bandoni<sup>1</sup>, Christian P. Robert<sup>1,2</sup>,, and Julien Stoehr<sup>1,3</sup>,

<sup>1</sup>CEREMADE, Université Paris-Dauphine, Université PSL, CNRS, 75016 Paris, France

<sup>2</sup>Department of Statistics, University of Warwick, Coventry CV4 7AL, UK

<sup>3</sup>Université Paris-Saclay, INRAE, AgroParisTech, UMR MIA Paris-Saclay, 91120 Palaiseau, France

## Abstract

Kernel quadrature is widely used to approximate integrals of smooth functions, with worst-case error typically decaying at the minimax rate  $n^{-\alpha/d}$  for smoothness  $\alpha$  in dimension  $d$ . Existing rate-optimal methods often depend on deterministic point sets tailored to a specific kernel, making them sensitive to misspecification and less robust in practice. In this work, we study randomized quadrature methods with a focus on robustness rather than kernel-specific optimality. We construct an explicit,  $n$ -dependent sampling distribution that achieves minimax rates for worst-case error over smoothness classes without requiring knowledge of the kernel. This kernel-agnostic design improves robustness while retaining optimal rates. Our analysis includes unbounded sampling measures such as Gaussian and Student- $t$  distributions, extending beyond compact domains. The results provide both theoretical guarantees and a practical recipe for robust, rate-optimal randomized quadrature.

**Keywords.** Probabilistic Integration, Bayesian Quadrature, Uncertainty Quantification, Contraction Rates, Minimax Rates

## 1 Introduction

Computing integrals is a fundamental task in modern statistics. Expectations, marginal likelihoods, posterior summaries, and predictive quantities are all expressed as integrals that rarely admit closed-form solutions. As a result, numerical integration plays a central role in both Bayesian and frequentist computation. In many contemporary applications, the integrand is expensive to evaluate and approximation error propagates through complex computational pipelines. In such settings, the choice of integration method directly impacts statistical accuracy.

Monte Carlo (MC) methods are widely used due to their simplicity, robustness, and dimension-independent convergence rate. The standard MC estimator achieves a root mean square error (RMSE) of order  $n^{-1/2}$ , regardless of dimension [Robert and Casella, 2004]. This makes MC particularly attractive in high-dimensional problems. However, in low and moderate dimensions the  $n^{-1/2}$  rate can be slow compared to methods that exploit additional structure such as smoothness.

Kernel-based quadrature methods, also known as Bayesian quadrature (BQ), provide a principled alternative grounded in function approximation [Hennig et al., 2022, Mahserici and Karvonen, 2026]. By placing a Gaussian process prior on the integrand [Rasmussen and Williams,

2006], BQ produces both a point estimate of the integral and a posterior distribution that quantifies epistemic uncertainty due to finite evaluations [Briol et al., 2019]. The resulting estimator can be written as a weighted sum of function evaluations at selected points, where the weights are determined by a positive-definite kernel and encode information about the integration measure.

Importantly, kernel quadrature should be viewed not merely as a refinement of Monte Carlo, but as a generalisation of classical deterministic cubature rules. For suitable choices of kernel and design points, the posterior mean recovers well-known numerical integration schemes such as the trapezoidal rule and Gauss–Hermite quadrature [Suldin, 1959, Särkkä et al., 2016, Karvonen and Särkkä, 2017]. In this sense, KQ provides a unifying probabilistic framework for classical quadrature, enriching these methods with uncertainty quantification and a functional-analytic interpretation. When the integrand possesses  $\alpha$  derivatives in dimension  $d$ , KQ can achieve convergence rates of order  $n^{-\alpha/d}$  [Novak, 1988], which can substantially outperform the Monte Carlo rate in smooth, low-dimensional settings.

Despite these attractive properties, a central and still poorly understood aspect of kernel quadrature is the choice of sampling distribution for the evaluation points. While much of the literature focuses on deterministic point sets obtained by variance minimisation [Briol et al., 2015, Osborne et al., 2012, Fisher et al., 2020b] or space-filling criteria [Briol et al., 2019, Kanagawa et al., 2020a, Fernández et al., 2020, Fisher et al., 2020a], randomized constructions offer improved robustness and practical flexibility [Briol et al., 2017]. For a given function class  $\mathcal{F}$  and distribution class  $\mathcal{P}$ , kernel  $k$ , and sample size  $n$ , one can formalise the problem of optimal sampling as the search for a distribution that minimises the worst-case RMSE over  $\mathcal{F}$  and  $\mathcal{P}$  [Briol et al., 2017]. However, in contrast to importance sampling, where an optimal proposal distribution can be characterised explicitly [Robert and Casella, 2004], no general closed-form solution is known for kernel quadrature, and limited theoretical guidance is available.

The challenge becomes particularly pronounced on unbounded domains. While minimax-optimal sampling strategies are known for smooth functions on bounded sets [Chen et al., 2025, Briol et al., 2019], many statistical applications involve Gaussian or heavy-tailed measures defined on the whole space  $\mathbb{R}^d$ . In such settings, existing constructions do not directly apply, and naive choices, such as sampling from the target distribution, can lead to significant inefficiencies [Briol et al., 2017]. Moreover, deterministic designs that depend strongly on precise kernel specification may suffer from a lack of robustness when smoothness assumptions are only approximately satisfied [Wynne et al., 2021, Kanagawa et al., 2020b].

The aim of this work is to analyse and construct randomized sampling strategies for kernel quadrature that achieve minimax-optimal convergence rates on unbounded domains. We provide an explicit,  $n$ -dependent sampling distribution that attains the optimal rate  $n^{-\alpha/d}$  over smoothness classes, while remaining kernel-agnostic and robust to misspecification. Our results clarify the role of sampling in kernel quadrature, extend minimax theory to unbounded settings relevant to statistics, and provide a principled and practical foundation for robust probabilistic integration.

**Outline** The paper is organized as follows. Section 3 provides background on BC and introduces an analytical framework for studying the proposed method, while also discussing relevant results and methodologies from the existing literature. In Section 4, we present our novel theoretical contributions, extending optimal sampling results to unbounded domains. Section 5 illustrates the practical utility of our framework through numerical experiments. Finally, Section 6 concludes the paper with a discussion of key findings and potential directions for future work.

## 2 Notations

Let  $f : \mathcal{X} \rightarrow \mathbb{R}$  be a function defined on  $\mathcal{X} \subset \mathbb{R}^d$ , and let  $\Pi$  be a Borel probability measure on  $\mathcal{X}$ . We denote by

$$\Pi(f) = \int_{\mathcal{X}} f(x) \Pi(dx)$$

the integral of  $f$  with respect to  $\Pi$ . For  $1 \leq p < \infty$ , we denote by  $\|f\|_{L^p(\mathcal{X}, \Pi)} = \left( \int_{\mathcal{X}} |f(x)|^p \Pi(dx) \right)^{1/p}$  the weighted  $L^p$ -norm of  $f$  on  $\mathcal{X}$  with respect to  $\Pi$ , and by  $\|f\|_{L^\infty(\mathcal{X})} = \text{ess sup}_{x \in \mathcal{X}} |f(x)|$  the  $L^\infty$  (essential supremum) norm of  $f$ . When the measure and domain are clear from context, we may simply write  $\|f\|_{L^p}$  or  $\|f\|_{L^\infty}$ . Moreover, let  $\mathcal{H}^\alpha(\mathcal{X})$  denote the Sobolev space of order  $\alpha \in \mathbb{N}_0$  on  $\mathcal{X}$ , equipped with the norm

$$\|f\|_{\mathcal{H}^\alpha(\mathcal{X})} = \left( \sum_{|\beta| \leq \alpha} \int_{\mathcal{X}} |D^\beta f(x)|^2 dx \right)^{1/2},$$

where  $\beta = (\beta_1, \dots, \beta_d)$  is a multi-index,  $|\beta| = \beta_1 + \dots + \beta_d$ , and  $D^\beta f = \frac{\partial^{|\beta|} f}{\partial x_1^{\beta_1} \dots \partial x_d^{\beta_d}}$  denotes the corresponding weak derivative. When the domain  $\mathcal{X}$  is clear from context, we will omit it and simply write  $\mathcal{H}^\alpha$ . Let  $k : \mathcal{X} \times \mathcal{X} \rightarrow \mathbb{R}$  be a symmetric, positive-definite kernel, the reproducing kernel Hilbert space (RKHS) associated with  $k$ , denoted by  $\mathcal{H}_k(\mathcal{X})$ , is the Hilbert space of functions  $f : \mathcal{X} \rightarrow \mathbb{R}$  such that  $f(x) = \langle f, k(x, \cdot) \rangle_{\mathcal{H}_k}$  for all  $x \in \mathcal{X}$ , where  $\langle \cdot, \cdot \rangle_{\mathcal{H}_k}$  is the inner product in  $\mathcal{H}_k(\mathcal{X})$ . The RKHS norm is defined as

$$\|f\|_{\mathcal{H}_k}^2 = \langle f, f \rangle_{\mathcal{H}_k} = \sum_{i,j} c_i c_j k(x_i, x_j)$$

for any finite linear combination  $f = \sum_i c_i k(x_i, \cdot)$ . Similarly, when the domain is clear, we will omit  $\mathcal{X}$  and write  $\mathcal{H}_k$ . Given a set of points  $\mathbf{x}_{1:n} = (x_1, \dots, x_n)$ ,  $x_i \in \mathcal{X}$  for  $i = 1, \dots, n$  and a compact domain  $\mathcal{X}$ , we define the fill distance as  $h_{\mathbf{x}_{1:n}, \mathcal{X}} = \sup_{x \in \mathcal{X}} \min_{1 \leq j \leq n} \|x - x_j\|_2$ , where  $\|\cdot\|_2$  is the Euclidean norm. Moreover, we distinguish different probabilistic versions of the big- $\mathcal{O}$  notation. For a sequence of random variables  $(X_n)_{n \geq 1}$  and a deterministic sequence  $(a_n)_{n \geq 1}$ , we write  $X_n = \mathcal{O}_{\mathbb{P}}(a_n)$  if  $X_n/a_n$  is bounded in probability, i.e., if for every  $\varepsilon > 0$ , there exists  $M > 0$  such that

$$\sup_{n \geq 1} \mathbb{P} \left[ \left| \frac{X_n}{a_n} \right| > M \right] \leq \varepsilon.$$

We refer to this notion as big- $\mathcal{O}$  in probability. In addition, we will also use a stronger high-probability version of this notation: we write  $X_n = \mathcal{O}_P(a_n)$  (with high probability) if there exist constants  $C, c > 0$  such that  $\mathbb{P}(|X_n| > Ca_n) \leq n^{-c}$ , which is a big- $\mathcal{O}$  notation with polynomially high probability. If instead, it further holds that  $\mathbb{P}(|X_n| > Ca_n) \leq e^{-cn}$ , we will write  $X_n \in \mathcal{O}_P(a_n)$  with exponentially high probability. Finally, we will use  $f$  to denote the integrand, viewed as an element of a generic function space, and  $f^*$  to denote its Gaussian process surrogate.

## 3 Background on Bayesian Quadrature

**Problem formulation** Consider approximating the Lebesgue integral  $\Pi(f) = \int_{\mathcal{X}} f d\Pi$ , where  $\Pi$  is a Borel probability measure on  $\mathcal{X} \subseteq \mathbb{R}^d$  and  $f$  is square-integrable with respect to  $\Pi$  and it is possible to compute exact evaluations. In Bayesian quadrature [Hennig et al., 2022], the integrand  $f$  is modeled as a Gaussian process  $f^* \sim \mathcal{GP}(0, k)$ , where  $k : \mathcal{X} \times \mathcal{X} \rightarrow \mathbb{R}$  is a symmetric, positive-definite kernel. Given evaluations  $\mathbf{f}_{1:n} = (f(x_1), \dots, f(x_n))^\top = (f^*(x_1), \dots, f^*(x_n))^\top = \mathbf{f}_{1:n}^*$  at design points  $\mathbf{x}_{1:n} = (x_1, \dots, x_n)^\top \in \mathcal{X}^n$ , the posterior distribution of the integral is

$$\Pi(f^*) \mid \mathbf{x}_{1:n} \sim \mathcal{N} \left( m_\Pi(\mathbf{x}_{1:n})^\top \mathbf{K}^{-1} \mathbf{f}_{1:n}, \Pi^{\otimes 2}(k) - m_\Pi(\mathbf{x}_{1:n})^\top \mathbf{K}^{-1} m_\Pi(\mathbf{x}_{1:n}) \right),$$

where  $\mathbf{K}$  is a symmetric positive definite matrix with  $\mathbf{K}_{ij} = k(x_i, x_j)$ , and

$$m_{\Pi}(\mathbf{x}_{1:n}) = (\Pi(k(\cdot, x_1)), \dots, \Pi(k(\cdot, x_n)))^{\top}$$

is the kernel mean vector. The posterior mean defines the weighted estimator

$$\widehat{\Pi}_n(f^*) = \sum_{j=1}^n w_j f(x_j), \quad \mathbf{w}_{1:n} = (w_1, \dots, w_n)^{\top} = \mathbf{K}^{-1} m_{\Pi}(\mathbf{x}_{1:n}),$$

where we recall that  $f(x_i) = f^*(x_i)$  for  $i = 1, \dots, n$  and some properties, like positivity and the magnitude of the BQ weights, can be recovered in some contexts [Karvonen et al. \[2019\]](#).

The RKHS [\[Berlinet and Thomas-Agnan, 2011\]](#) provides a clean interpretation of integration error. The kernel mean embedding  $\mu_{\Pi} \in \mathcal{H}_k$  satisfies  $\Pi(f^*) = \langle f, \mu_{\Pi} \rangle_{\mathcal{H}_k}$  for all  $f \in \mathcal{H}_k$ , and the estimator  $\widehat{\Pi}_n(f^*)$  corresponds to replacing  $\mu_{\Pi}$  by the empirical element  $\mu_n = \sum_{j=1}^n w_j k(\cdot, x_j)$ . The posterior variance then coincides with the squared worst-case integration error over the unit ball of  $\mathcal{H}_k$ ,

$$\text{Var}_{f^*}[\Pi(f^*) \mid \mathbf{x}_{1:n}] = \|\mu_{\Pi} - \mu_n\|_{\mathcal{H}_k}^2 = \sup_{\|f\|_{\mathcal{H}_k} \leq 1} |\Pi(f) - \widehat{\Pi}_n(f)|^2,$$

with weights that minimize the worst case error [Karvonen et al. \[2019\]](#), providing a principled, kernel-encoded measure of remaining integration uncertainty. This variational characterization has motivated a substantial line of work on the construction of point sets that directly minimize  $\|\mu_{\Pi} - \mu_n\|_{\mathcal{H}_k}$ . Deterministic approaches include greedy sequential minimisation of the posterior variance: [Briol et al. \[2015\]](#), [Wagstaff et al. \[2018\]](#), [Simpson et al. \[2021\]](#), [Adachi et al. \[2022\]](#) selected evaluation points using the Frank–Wolfe algorithm, while providing provable theoretical convergence guarantees on the integration error. [Osborne et al. \[2012\]](#), [Gunter et al. \[2014\]](#) developed Bayesian quadrature methods that actively select evaluation points to estimate model evidence and posterior quantities, where convergence guarantees for a broad class of such adaptive Bayesian quadrature methods are established by [Kanagawa and Hennig \[2019\]](#). On the randomized side, [Bach \[2017\]](#) provided strong theoretical guarantees for a specially constructed sampling distribution using the Mercer decomposition of the kernel, but in practice this distribution may be difficult to compute. A more recent line of work exploits determinantal point processes (DPPs) as a randomized design strategy [Belhadji et al. \[2019\]](#): since DPPs are repulsive by construction, samples from a DPP associated with the kernel  $k$  tend to spread across  $\mathcal{X}$  in a way that controls the fill distance. These constructions, however, require to efficiently sample from the associated DPP, which can be computationally prohibitive. Finally, [Hayakawa et al. \[2022\]](#) proposed kernel quadrature methods that enforce positive integration weights by selecting a subsample from an initial large set of points, aiming to improve numerical stability while retaining accuracy, and provides theoretical error guarantees. However, it requires explicit knowledge of the Mercer decomposition of the kernel, which is not available in general contexts.

**Fill Distance and Convergence Rates** When  $\mathcal{H}_k$  is norm-equivalent to a Sobolev space  $\mathcal{H}^{\alpha}$  of smoothness  $\alpha > d/2$ , the minimax integration error over this class decays at the rate  $n^{-\alpha/d}$  [\[Novak, 1988\]](#). The geometric mechanism through which the placement of design points enters this bound is captured by the fill distance which measures the radius of the largest ball in  $\mathcal{X}$  containing no design point. Results from scattered data approximation [\[Wendland, 2004\]](#) show that the kernel interpolant  $s_n$  of any  $f \in \mathcal{H}_k(\mathcal{X})$ , where  $\mathcal{X}$  is compact and satisfies the interior cone condition, satisfies

$$\|f - s_n\|_{L^{\infty}} \leq C h_{\mathbf{x}_{1:n}, \mathcal{X}}^{\alpha} \|f\|_{\mathcal{H}_k},$$

for some constant  $C$ , which directly implies that  $\|\mu_{\Pi} - \mu_n\|_{\mathcal{H}_k} \leq C h_{\mathbf{x}_{1:n}, \mathcal{X}}^{\alpha}$ . Controlling optimally the fill distance is therefore sufficient to achieve optimal rates.

**Existing Guarantees on Bounded Domains** The interplay between fill distance and sampling distribution was made precise by Briol et al. [2019] for the case  $\mathcal{X} = [0, 1]^d$ . If the design points are generated by a uniformly ergodic Markov chain targeting  $\Pi$ , a covering argument yields  $h_{\mathbf{x}_{1:n}, \mathcal{X}} = \mathcal{O}_{\mathbb{P}}(n^{-1/d+\varepsilon})$  in probability for any  $\varepsilon > 0$ , from which the worst-case error satisfies

$$\|\mu_{\Pi} - \mu_n\|_{\mathcal{H}_k} = \mathcal{O}_{\mathbb{P}}(n^{-\alpha/d+\varepsilon}).$$

This establishes that MCMC-based Bayesian quadrature attains the minimax-optimal rate  $n^{-\alpha/d}$  up to an arbitrarily small logarithmic correction, and moreover that the posterior contracts to the true integral at a super-exponential rate. Importantly, the proof proceeds entirely through control of the fill distance and does not require the design to be tailored to the specific kernel: the sampling distribution alone determines the geometry, and optimality follows as a consequence.

This result, however, is confined to compact domains  $\mathcal{X}$  in  $\mathbb{R}^d$ , by smoothly reparametrizing  $\mathcal{X}$  in  $[0, 1]^d$ . Many statistical applications involve measures with unbounded support, such as Gaussian or heavy-tailed distributions on  $\mathbb{R}^d$ , for which the fill distance framework does not directly apply: the domain cannot be covered by finitely many balls of a fixed radius  $h$ , and naive sampling from the target can concentrate mass in high-probability regions while leaving large portions of the effective support underexplored. The sensitivity of the sampling distribution was demonstrated empirically by Briol et al. [2017], who showed that even moderate misspecification of the proposal leads to substantial deterioration of the root mean square error, independently of the asymptotic rate.

## 4 Theoretical Guarantees for Unbounded Domains

### 4.1 The Challenge of Unbounded Domains

A natural approach to extending the guarantees of Briol et al. [2019] to unbounded domains is to map the problem back to  $[0, 1]^d$  using a change of variables. Let  $T$  denote the inverse cumulative distribution function (CDF) associated with the measure  $\Pi$ . Then the integral can be rewritten as

$$\int_{\mathcal{X}} f(x) d\Pi(x) = \int_{[0,1]^d} f(T(u)) du = \int_{[0,1]^d} \tilde{f}(u) du.$$

If  $\tilde{f}$  belongs to an RKHS  $\mathcal{H}$  that is norm-equivalent to a Sobolev space of order  $\alpha$ , then Theorem 1 of Briol et al. [2019] applies directly and the rate  $n^{-\alpha/d}$  is recovered. However, this requirement typically fails in unbounded settings, even in simple cases such as when  $\Pi$  is the standard Gaussian measure on  $\mathbb{R}$ . To illustrate this, consider the following example.

**Example** Let  $f(x) = x$ , which is infinitely smooth ( $f \in C^\infty(\mathbb{R})$ ), and let  $\Pi$  be the standard Gaussian measure on  $\mathbb{R}$ . In this case,  $\tilde{f}(u) = f(\Phi^{-1}(u)) = \Phi^{-1}(u)$ , where  $\Phi$  denotes the standard Gaussian CDF. The first derivative of  $\tilde{f}$  is given by  $\tilde{f}'(u) = \frac{1}{\phi(\Phi^{-1}(u))}$ , where  $\phi$  is the standard Gaussian density. The  $L^2$ -norm of  $\tilde{f}'$  is given by

$$\int_0^1 |\tilde{f}'(u)|^2 du = \int_0^1 \frac{1}{[\phi(\Phi^{-1}(u))]^2} du = \int_{-\infty}^{\infty} \frac{1}{\phi(x)} dx = \infty.$$

Hence,  $\tilde{f} \in L^2(0, 1)$ , but  $\tilde{f} \notin H^1([0, 1])$  and, as a result, applying Theorem 1 of Briol et al. [2019] to the transformed problem yields convergence rates no faster than  $\mathcal{O}(n^{-1+\varepsilon})$ , against the theoretical  $\mathcal{O}(n^{-\alpha})$ , for any  $\alpha \geq 1$ .

This represents a catastrophic loss of regularity: a smooth function  $f \in \mathcal{H}^\alpha$  on  $\mathbb{R}$  is transformed into  $\tilde{f}$  on  $[0, 1]$  whose regularity is independent of  $\alpha$ , destroying the fast convergence rates that kernel quadrature is designed to achieve. Obtaining analogous posterior contraction

results for integration over unbounded domains therefore requires a different approach. Rather than transforming the domain, we work directly on  $\mathcal{X} = \mathbb{R}^d$  and construct a sampling distribution that controls the fill distance in a way that respects both the tail behaviour of  $\Pi$  and the smoothness encoded by  $\mathcal{H}_k$ . Our main result establishes that this is possible.

## 4.2 Optimal Sampling on Unbounded Domains

As in Briol et al. [2019], we make a slight strengthening of the assumption on the kernel:  $C_k := \sup_{x \in \mathcal{X}} k(x, x) < \infty$ . This implies that all  $f \in \mathcal{H}_k$  are bounded on  $\mathcal{X}$ . Our main theoretical contribution is the following theorem, whose proof is provided in Appendix A.

**Theorem 1.** *Let  $\mathcal{X} = \mathbb{R}^d$  and let  $\mathcal{H}_k$  be a reproducing kernel Hilbert space norm-equivalent to the Sobolev space  $\mathcal{H}^\alpha(\mathbb{R}^d)$  with  $\alpha > d/2$ . Suppose  $x_1, \dots, x_n$  are sampled independently from a proposal distribution  $Q_n$ , and the target measure  $\Pi$  is either Gaussian or Student. Then, for any  $f \in \mathcal{H}_k$  and for any  $\varepsilon > 0$ ,  $\delta > 0$ , there exists  $C_\delta > 0$  such that  $\|\mu_\Pi - \mu_n\|_{\mathcal{H}_k} = \mathcal{O}_P(n^{-\alpha\tau+\varepsilon})$  and*

$$\mathbb{P}[|\Pi(f^*) - \Pi(f)| < \delta \mid \mathbf{x}_{1:n}] = 1 - \mathcal{O}_P(\exp(-C_\delta n^{2\alpha\tau-\varepsilon})),$$

where  $\tau$  is defined as follows

(i) For the Gaussian target  $\Pi = \mathcal{N}(0, I_d)$ , and  $Q_n = \mathcal{N}(0, \Sigma_n)$  with  $\Sigma_n \asymp (\alpha \log n) I_d$ , then  $\tau = 1/d$ .

(ii) For the Student- $t$  target  $\Pi = t_\nu(0, I_d)$  with  $\nu$  degrees of freedom, and  $Q_n = t_\nu(0, \Sigma_n)$  with  $\Sigma_n \asymp n^{2\alpha\tau/(\nu+d/2)} I_d$ , then

$$\tau = \frac{\nu + d/2}{d(\alpha + \nu + d/2)}.$$

Several remarks are in order. First, the rate  $n^{-\alpha/d+\varepsilon}$  matches the minimax-optimal rate for integration in Sobolev spaces of smoothness  $\alpha$  in dimension  $d$  up to an  $\varepsilon > 0$  arbitrarily small, recovering the bound of Briol et al. [2019]. Second, the sampling distribution is explicit and  $n$ -dependent: the variance  $\Sigma_n \asymp \log n I_d$ , where  $\alpha$  can be dropped providing the same rates, ensures that the effective support of the sampling distribution grows with  $n$  at a rate that balances the decay of  $\Pi$  in the tails against the need to cover the domain where  $f$  may have significant mass. Third, the result is kernel-agnostic: the sampling distribution depends only on the target measure  $\Pi$ , not on the specific kernel  $k$  within the Sobolev equivalence class. The construction extends immediately to general Gaussian measures  $\Pi = \mathcal{N}(\mu, \Sigma)$  via the linear change of variables  $x = \mu + \Sigma^{1/2}y$ , which preserves smoothness. The optimal sampling distribution is then  $\mathcal{N}(\mu, (\log n)\Sigma)$ , a Gaussian with the same mean as  $\Pi$  and covariance scaled by  $\log n$ .

Several remarks are in order also for the Student- $t$  case. First, the rate  $n^{-\alpha(\nu+d/2)/(d(\alpha+\nu+d/2))+\varepsilon}$  interpolates naturally between heavy and light tails: as  $\nu \rightarrow \infty$  the exponent recovers  $-\alpha/d + \varepsilon$ , matching the Gaussian rate, while small  $\nu$  reflects the genuine difficulty of integrating against heavy-tailed distributions. Second, unlike the Gaussian case where  $\alpha$  enters the sampling variance only as a multiplicative factor and can be absorbed into the asymptotic constant, here  $\alpha$  appears in the exponent of  $\Sigma_n \asymp n^{2\alpha/(d(\alpha+\nu+d/2))} I_d$ , so the sampling distribution depends explicitly on  $\alpha$  and a careful choice of the smoothness parameter is required. Third, the result can be extended beyond Student- $t$  targets via a change of measure. Suppose the target distribution  $\Pi$  has polynomially decaying tails with a known rate. We introduce an auxiliary distribution  $t_\nu(0, I_d)$  whose tails are heavier than those of  $\Pi$ , and rewrite  $\Pi(f) = \mathbb{E}_{t_\nu}[f(x)w(x)]$ , where  $w = \frac{d\Pi}{dt_\nu}$ . The requirement is that the function  $g = fw$  belongs to the reproducing kernel Hilbert space  $\mathcal{H}_k$ , which is ensured if  $w \in \mathcal{H}_k$ . Now suppose that  $f$  is locally Sobolev of order  $\alpha$ , has finite

$L^\infty(\mathbb{R}^d)$ -norm, but does not decay at infinity. In this case, we instead use a Student- $t$  distribution with fewer degrees of freedom,  $t_{\nu-d/2-\varepsilon}$ . Writing  $g = f \cdot \frac{t_\nu}{t_{\nu-d/2-\varepsilon}}$ , we obtain  $g \in \mathcal{H}^\alpha(\mathbb{R}^d)$  for any  $\varepsilon > 0$ . Consequently, integration under  $t_{\nu-d/2-\varepsilon}$  achieves the convergence rate  $n^{-\alpha\nu/(d(\alpha+\nu))+\varepsilon}$ . Conversely, if the mass of  $f$  decays at infinity faster than required for  $L^2$ -integrability, one can choose a proposal distribution with lighter tails, thereby improving the effective regularity of  $g$  and potentially accelerating convergence.

The requirement that samples be drawn from a Gaussian with time-varying variance can be relaxed to allow for a sequential sampling scheme, as the following corollary shows.

**Corollary 2.** *Under the hypotheses of Theorem 1, suppose  $\mathbf{x}_{1:n} = (x_1, \dots, x_n)$  are independent points such that  $x_i \sim Q_i$  according to Theorem 1, where  $\Sigma_i \asymp s(i) I_d$ , with*

- (i)  $s(i) \asymp \log i$  in the Gaussian target case,
- (ii)  $s(i) \asymp i^{2\alpha/(d(\alpha+\nu+d/2))}$  in the Student- $t$  target case.

Then the same rates as in Theorem 1 hold.

### 4.3 Minimax Optimality for the Student- $t$ Target

Theorem 1 establishes that the sampling distribution  $Q_n = t_\nu(0, \Sigma_n)$  with  $\Sigma_n \asymp n^{\frac{2\alpha}{d(\alpha+\nu+d/2)}} I_d$  achieves worst-case integration error  $\mathcal{O}_P(n^{-\frac{\alpha(\nu+d/2)}{d(\alpha+\nu+d/2))+\varepsilon})$  in the case of a Student- $t$  target. We now show that it is the minimax rate up to the  $\varepsilon$ -correction. The proof of the Theorem is deferred to Appendix A.

**Theorem 3.** *Let  $\alpha > d/2$ ,  $\nu > 0$ ,  $R \geq 1$ , and let  $p_\nu : \mathbb{R}^d \rightarrow (0, \infty)$  satisfy*

$$c_1(1 + \|x\|_2^2)^{-(\nu+d)/2} \leq p_\nu(x) \leq c_2(1 + \|x\|_2^2)^{-(\nu+d)/2}.$$

There exists  $c > 0$  such that for any  $n \in \mathbb{N}$ , for any quadrature rule with  $n$  nodes  $Q \in \mathcal{Q}_n$ , the minimax quadrature error over the unit ball in  $H^\alpha(\mathbb{R}^d)$  satisfies:

$$\mathcal{E}_n = \inf_{Q \in \mathcal{Q}_n} \sup_{\|f\|_{H^\alpha} \leq 1} \left| \int_{\mathbb{R}^d} f(x) p_\nu(x) dx - \sum_{i=1}^n w_i f(x_i) \right| \geq c n^{-\frac{\alpha(\nu+d/2)}{d(\alpha+\nu+d/2)}}.$$

In the Gaussian case, a similar argument yields the classical bounded case rate  $n^{-s/d}$  up to logarithmic factors. More broadly, the techniques used in the proof of the lower bound can also be employed to show the suboptimality of the strategy that samples directly from the target measure in unbounded domains. This contrasts with the case of bounded domains, where such a strategy can achieve the optimal rate. The arguments are particularly well-suited to measures with radial densities. In this case, balls are extremal in the sense that they minimize volume for a given radius while simultaneously capturing the largest possible mass. This property allows the error analysis to be reduced to estimates over balls. For more general measures, such a reduction need not hold, and the geometry of optimal sets can be considerably more complex. Finally, the  $\varepsilon$ -loss in the upper bound is due to random sampling. A quasi-uniform design restricted to the relevant region, namely a ball centered at the origin with radius  $n^{\frac{\alpha}{d(\alpha+\nu+d/2)}}$ , would yield the sharp minimax rate without the  $\varepsilon$ -correction. However, such constructions would be practically not stable.

## 4.4 Posterior Variance Decomposition

Let  $\mathbf{f}_{1:n} = (f(x_1), \dots, f(x_n))^\top$  be the evaluations at  $\mathbf{x}_{1:n} = (x_1, \dots, x_n)^\top$  sampled independently from a proposal distribution  $Q$ . Then, by the law of total variance, the overall variance can be decomposed as

$$\text{Var}_{f^*, \mathbf{x}_{1:n}} [\Pi(f^*)] = \mathbb{E}_{\mathbf{x}_{1:n}} [\text{Var}_{f^*} [\Pi(f^*) \mid \mathbf{x}_{1:n}]] + \text{Var}_{\mathbf{x}_{1:n}} [\mathbb{E}_{f^*} [\Pi(f^*) \mid \mathbf{x}_{1:n}]].$$

The first term corresponds to the expected posterior variance, conditioned on the sampled locations, which can be controlled using Theorem 1, by boundedness of the posterior variance and that convergence results hold with high probability. The second term captures the additional variability introduced by the randomness of the nodes  $\mathbf{x}_{1:n}$  themselves. This decomposition highlights that convergence rates established in Theorem 1 must account not only for the posterior variance, but also for the stochasticity of the point selection process. Intuitively, these two terms can be controlled by the expected posterior variance and the norm of  $f$ . To formalize this intuition, we present the following proposition, whose proof is deferred to Appendix A.

**Proposition 4.** *Let  $f \in \mathcal{H}^\alpha$ , with  $\mathcal{H}^\alpha$  norm-equivalent to the RKHS  $\mathcal{H}_k$  associated with kernel  $k$ . Let  $\Pi(f^*) \mid \mathbf{x}_{1:n}$  denote the Bayesian quadrature posterior of the integral based on  $n$  points  $\mathbf{x}_{1:n} = (x_1, \dots, x_n)^\top$  sampled from a proposal distribution  $Q$ . Then there exists a constant  $C > 0$  such that*

$$\text{Var}_{f^*, \mathbf{x}_{1:n}} [\Pi(f^*)] \leq C(1 + \|f\|_{\mathcal{H}^\alpha}^2) \mathbb{E}_{\mathbf{x}_{1:n}} [\text{Var}_{f^*} [\Pi(f^*) \mid \mathbf{x}_{1:n}]].$$

Combining Proposition 4 with the convergence rates of Theorem 1, we obtain a characterization of the rate at which the posterior variance of the Bayesian quadrature integral decays, considering uncertainty arising both from the Gaussian process  $f$  and from the random selection of points. The result is formalized in the following Corollary, with the proof provided in Appendix A.

**Corollary 5.** *Under the assumptions of Theorem 1, the posterior variance of  $\Pi(f^*)$  for  $f \in \mathcal{H}_k$ , norm-equivalent to the Sobolev space  $\mathcal{H}^\alpha$ , satisfies:*

$$\text{Var}_{f^*, \mathbf{x}_{1:n}} [\Pi(f^*)] = \mathcal{O}(n^{-2\alpha\tau+\varepsilon}),$$

where  $\tau$  is as defined in Theorem 1.

## 5 Numerical Experiments

We consider the integration problem  $\Pi(f) = \int_{\mathbb{R}} f(x) \Pi(dx)$ , where  $\Pi = \mathcal{N}(0, 1)$  is the standard Gaussian measure and  $f(x) = \sqrt{3}e^{-x^2} + \sin(2\pi x)/(1+x^2)$ , similarly to Briol et al. [2017] but which decays at infinity in order to have a function in  $\mathcal{H}^\alpha(\mathbb{R}^d)$ , for any  $\alpha \geq 1$ . We model  $f$  with a Gaussian process prior  $f^* \sim \mathcal{GP}(0, k)$ , using a Radial Basis Function (RBF) kernel [Rasmussen and Williams, 2006]:

$$k(x, x') = \sigma_f^2 \exp\left(-\frac{(x-x')^2}{2\ell^2}\right),$$

where  $\ell > 0$  is the lengthscale and  $\sigma_f^2 > 0$  the prior variance. Since both the kernel and the measure are Gaussian, the kernel mean

$$m_\Pi(x) = \int_{\mathbb{R}} k(x, x') d\Pi(x') = \sigma_f^2 \sqrt{\frac{\ell^2}{\ell^2 + 1}} \exp\left(-\frac{x^2}{2(\ell^2 + 1)}\right)$$

is available in closed form. Similarly, the prior variance of the integral

$$\text{Var}[\Pi(f^*)] = \int_{\mathbb{R}} \int_{\mathbb{R}} k(x, x') d\Pi(x) d\Pi(x') = \sigma_f^2 \sqrt{\frac{\ell^2}{\ell^2 + 2}}$$

is also analytic in this Gaussian–Gaussian setting, see table 10.1 in Hennig et al. [2022] for a non-exhaustive list of distribution and kernel that provide a closed-form expression for both the kernel mean and the prior variance. The lengthscale  $\ell$  controls the smoothness of the prior: smaller values allow faster variation, while larger values enforce smoother functions, whereas the signal variance  $\sigma_f^2$  sets the overall scale of variability, determining the magnitude of prior and posterior uncertainty.

## 5.1 Hyperparameter Estimation

Let  $\theta := (\sigma_f^2, \ell) \in (0, \infty)^2$  and  $\mathbf{x}_{1:n} = (x_1, \dots, x_n) \stackrel{\text{i.i.d.}}{\sim} \mathcal{N}(0, \log n) = Q_n$  according to Theorem 1. Denote by  $K_\theta = \sigma_f^2 K_\ell$ , with  $[K_\ell]_{i,j} = \exp\left(-\frac{(x_i - x_j)^2}{2\ell^2}\right)$ . We place priors  $\sigma_f^2 \sim \text{IG}(\alpha_f, \beta_f)$  and  $\ell \sim p(\ell)$ . Our goal is to characterize the full conditional marginals. By Bayes' formula, the conditional posterior of  $\sigma_f^2$  given  $\ell$  and observations  $\mathbf{f}_{1:n}$  is

$$p(\sigma_f^2 \mid \mathbf{f}_{1:n}, \ell) \propto p(\mathbf{f}_{1:n} \mid \sigma_f^2, \ell) p(\sigma_f^2).$$

Letting  $Q = \mathbf{f}_{1:n}^\top K_\ell^{-1} \mathbf{f}_{1:n} / 2$ , we obtain

$$\begin{aligned} p(\sigma_f^2 \mid \mathbf{f}_{1:n}, \ell) &\propto (\sigma_f^2)^{-n/2} \exp\left(-\frac{Q}{\sigma_f^2}\right) (\sigma_f^2)^{-(\alpha_f+1)} \exp\left(-\frac{\beta_f}{\sigma_f^2}\right) \\ &\propto (\sigma_f^2)^{-(\alpha_f+n/2+1)} \exp\left(-\frac{\beta_f + Q}{\sigma_f^2}\right), \end{aligned}$$

which corresponds to an inverse-gamma distribution  $\text{IG}(\alpha_f + n/2, \beta_f + Q)$ . Similarly, the full conditional of  $\ell$  is

$$p(\ell \mid \mathbf{f}_{1:n}, \sigma_f^2) \propto p(\mathbf{f}_{1:n} \mid \sigma_f^2, \ell) p(\ell) \propto p(\ell) |K_\ell|^{-1/2} \exp\left(-\frac{Q}{\sigma_f^2}\right),$$

which does not have a closed form and can be sampled efficiently using a Metropolis–Hastings step.

**Proposition 6.** *Let  $\theta = (\sigma_f^2, \ell) \in (0, \infty)^2$  and consider the posterior*

$$\pi(\sigma_f^2, \ell \mid \mathbf{f}_{1:n}) \propto p(\mathbf{f}_{1:n} \mid \sigma_f^2, \ell) p(\sigma_f^2) p(\ell),$$

where  $p(\sigma_f^2) = \text{IG}(\alpha_f, \beta_f)$  and  $p(\ell)$  is a proper, continuous prior on  $(0, \infty)$ . At each iteration, the sampler alternates between

$$\sigma_f^2 \mid \ell, \mathbf{f}_{1:n} \sim \text{IG}(\alpha_f + n/2, \beta_f + Q), \quad Q = \frac{1}{2} \mathbf{f}_{1:n}^\top K_\ell^{-1} \mathbf{f}_{1:n},$$

and a Metropolis–Hastings update for  $\ell$  with invariant density

$$\pi(\ell \mid \sigma_f^2, \mathbf{f}_{1:n}) \propto p(\ell) |K_\ell|^{-1/2} \exp(-Q/\sigma_f^2),$$

using any proposal  $q(\ell, \ell') > 0$  on  $(0, \infty)^2$ . Then the resulting chain  $\{\theta_t\}$  is aperiodic, Harris recurrent, and ergodic with invariant distribution  $\pi(\sigma_f^2, \ell \mid \mathbf{f}_{1:n})$ .

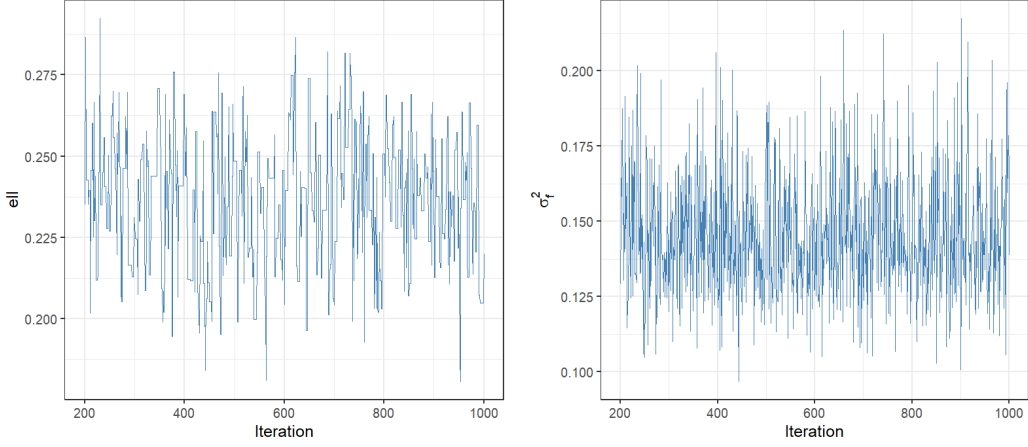


**Figure 1:** Trace plots of the Gaussian kernel hyperparameters obtained via a Metropolis-within-Gibbs sampler with  $n = 100$  points. A Markov chain of  $T = 1000$  iterations was generated, with the first 200 samples discarded as burn-in, leaving 800 retained samples shown. The left panel displays the trace of the length-scale parameter  $\ell$ , sampled using a random-walk Metropolis–Hastings step with proposal step size  $s_\ell = 0.2$  and acceptance rate of approximately 0.55 and a log-Normal prior with zero mean and variance 100. The right panel shows the trace of the signal variance  $\sigma_f^2$ , sampled directly from its conditional inverse-gamma distribution due to conjugacy with inverse-gamma parameters  $\alpha_f = \beta_f = 2$ .

To ensure positivity of  $\ell$  and improve numerical stability, the MH proposal is performed on the log-transformed variable  $u_\ell = \log(\ell)$ . At iteration  $t$ , let  $\ell_{\text{curr}} = \ell^{(t-1)}$  be the current value and define  $u_{\ell, \text{curr}} = \log(\ell_{\text{curr}})$ . A proposal is generated as

$$u_{\ell, \text{prop}} = u_{\ell, \text{curr}} + \epsilon, \quad \epsilon \sim \mathcal{N}(0, s_\ell^2),$$

and the corresponding proposed  $\ell$  is  $\ell_{\text{prop}} = \exp(u_{\ell, \text{prop}})$ . Since the proposal is made on the transformed scale, the posterior density must include a Jacobian adjustment for the change of variables. Specifically, if  $p(\ell \mid \mathbf{f}_{1:n}, \sigma_f^2)$  is the posterior density in the original scale, the density in the log scale is  $p(u_\ell \mid \mathbf{f}_{1:n}, \sigma_f^2) = p(\ell \mid \mathbf{f}_{1:n}, \sigma_f^2) \left| \frac{d\ell}{du_\ell} \right| = p(\ell \mid \mathbf{f}_{1:n}, \sigma_f^2) \cdot e^{u_\ell}$ . Taking logarithms, this results in the additional term  $u_\ell$  in the log posterior. Therefore, the log posterior for the proposed value is computed as

$$\log p(u_{\ell, \text{prop}} \mid \mathbf{f}_{1:n}, \sigma_f^{2(t-1)}) = -\frac{n}{2} \log \sigma_f^{2(t-1)} - \frac{1}{2\sigma_f^{2(t-1)}} \mathbf{f}_{1:n}^\top K_{\ell_{\text{prop}}}^{-1} \mathbf{f}_{1:n} + \log p(\ell_{\text{prop}}) + u_{\ell, \text{prop}},$$

and similarly for the current value. The MH acceptance probability is then

$$\alpha = \min \left\{ 1, \exp \left( \log p(u_{\ell, \text{prop}} \mid \cdot) - \log p(u_{\ell, \text{curr}} \mid \cdot) \right) \right\}.$$

The proposal  $\ell_{\text{prop}}$  is accepted with probability  $\alpha$ , otherwise the current value is retained. This procedure guarantees that the sampler targets the correct posterior while enforcing  $\ell > 0$ . After updating  $\ell$ , the full conditional of  $\sigma_f^2$  is used to sample the next value. Given the updated  $\ell^{(t)}$ , the kernel matrix  $K_\ell$  is computed, and  $\sigma_f^{2(t)}$  is drawn from an inverse-gamma distribution with shape parameter  $\alpha_f + n/2$  and scale parameter  $\beta_f + \frac{1}{2} \mathbf{f}_{1:n}^\top K_\ell^{-1} \mathbf{f}_{1:n}$ . In practice, a Cholesky decomposition of  $K_\ell$  is used to efficiently compute both  $K_\ell^{-1} \mathbf{f}_{1:n}$  and the log-determinant required in the posterior computation. A small nugget  $\eta I_n$ ,  $\eta = 10^{-8}$  is added to  $K_\ell$  for numerical stability and this procedure is iterated for  $T$  steps producing posterior samples  $\{\ell^{(t)}, \sigma_f^{2(t)}\}_{t=1}^T$ .

## 5.2 Bayesian Quadrature Posterior Computation

After obtaining posterior samples of the kernel hyperparameters  $\{\ell^{(t)}, \sigma_f^{2(t)}\}_{t=1}^T$ , we fix the RBF kernel parameters to their posterior averages

$$\bar{\theta}_T = (\bar{\sigma}_{f,T}^2, \bar{\ell}_T) = \frac{1}{T - T_0} \sum_{t=T_0+1}^T \theta^{(t)},$$

where  $T_0$  denotes the burn-in period. Using these fixed hyperparameters, we draw a set of design points  $\mathbf{x}_{1:n} = (x_1, \dots, x_n)$   $\overset{\text{i.i.d.}}{\sim} \mathcal{N}(0, \log n)$ , and compute the conditional posterior of the integral  $\Pi(f^*) \mid \mathbf{x}_{1:n}$ . Figure 2 compares the performance of two sampling strategies: a standard Gaussian distribution (measure of the integral) and the distribution  $Q_n$  of Theorem 1. In the left panel, the posterior mean obtained with the distribution  $Q_n$  approaches the true integral value more rapidly than in the standard Gaussian case. The corresponding uncertainty bands also contract faster, indicating a more efficient reduction of uncertainty. This difference is even more pronounced in the right panel. The posterior variance decreases substantially faster when using  $Q_n$ . After 150 evaluations, the variance is approximately  $1.01 \times 10^{-11}$ , whereas sampling from the standard Gaussian results in a final variance of  $1.57 \times 10^{-6}$ .

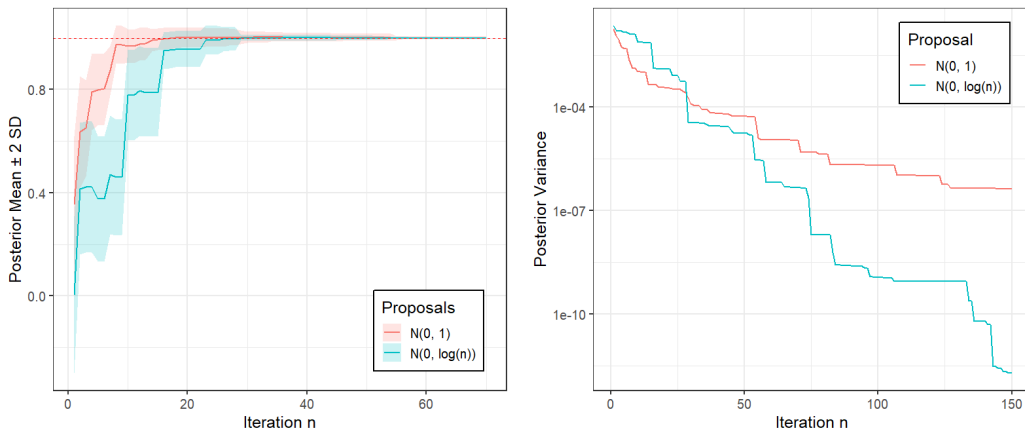


**Figure 2:** Left: posterior mean (solid lines) with  $\pm 2$  standard deviation bands over 70 sequential design iterations for two sampling strategies: standard Gaussian and  $Q_n$ ; the true integral value is shown as a dashed red line. Right: posterior variance (log scale) versus the number of evaluations for both strategies.

To propagate uncertainty from both the integrand and the random design, we repeat the experiment  $N$  times. Let  $\hat{\Pi}^{(i)}(f^*)$  and  $\hat{V}_n^{(i)}(f^*)$  denote the posterior mean and variance of  $\Pi(f^*)$  in the  $i$ -th repetition. The overall posterior mean and variance are estimated via

$$\bar{\Pi}_N(f^*) = \frac{1}{N} \sum_{i=1}^N \hat{\Pi}^{(i)}(f^*), \quad \bar{V}_N(f^*) = \frac{1}{N} \sum_{i=1}^N \hat{V}_n^{(i)}(f^*) + \frac{1}{N} \sum_{i=1}^N (\hat{\Pi}^{(i)}(f^*) - \bar{\Pi}_N(f^*))^2,$$

where the second term captures variability due to the randomness of the design points, in accordance with the law of total variance. More formally, let  $p(\Pi(f^*), \mathbf{x}_{1:n})$  be the joint distribution of the integral and the design points. For a fixed  $\mathbf{x}_{1:n}$ , the conditional posterior  $p(\Pi(f^*) \mid \mathbf{x}_{1:n})$  is Gaussian, but marginalizing over the random design yields a non-Gaussian mixture:

$$p(\Pi(f^*)) = \int p(\Pi(f^*) \mid \mathbf{x}_{1:n}) p(\mathbf{x}_{1:n}) d\mathbf{x}_{1:n} \approx \frac{1}{R} \sum_{i=1}^R \mathcal{N}(\hat{\Pi}^{(i)}(f^*), \hat{V}_n^{(i)}(f^*)),$$

where  $R$  independent sets of design points are used, and each Gaussian component corresponds to the posterior conditional on one sampled design. Because the component means and variances vary, the mixture is generally non-Gaussian.

Credible intervals for  $\Pi(f^*)$  are obtained by Monte Carlo sampling from this mixture. Specifically, for each component  $i$ , we draw  $S$  independent samples:

$$Z_{i,s} = \hat{\Pi}^{(i)}(f^*) + \sqrt{\hat{V}_n^{(i)}(f^*)} \varepsilon_{i,s}, \quad \varepsilon_{i,s} \sim \mathcal{N}(0, 1), \quad s = 1, \dots, S.$$

The combined set of  $R \cdot S$  samples  $\{Z_{i,s}\}_{i=1, \dots, R; s=1, \dots, S}$  provides an empirical approximation of the marginal posterior. Empirical quantiles of these samples then yield credible intervals, giving a distribution-free summary that simultaneously accounts for uncertainty in the Gaussian process model and the randomness of the design points. Figure 3 shows results averaged over  $N = 1,000$  independent repetitions and  $S = 100$  independent samples for the same two sampling strategies. In the left panel, the posterior mean for  $Q_n$  approaches the true integral value more quickly, with 95% uncertainty bands contracting faster, while being larger at early iterations than in the Gaussian case. In the right panel, the total posterior variance decreases smoothly for both strategies, but  $Q_n$  achieves a much lower variance more rapidly. At the final iteration, the variance is approximately  $5.87 \times 10^{-9}$  for  $Q_n$ , compared to  $4.26 \times 10^{-6}$  for the standard Gaussian, highlighting the efficiency gain from using  $Q_n$ .

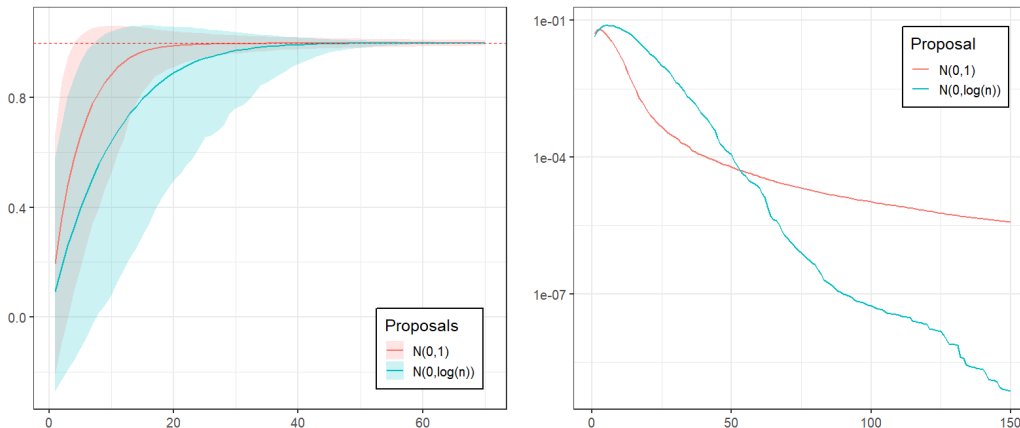


**Figure 3:** Left: average posterior mean (solid lines) with 95% uncertainty bands over sequential design iterations, computed from 1,000 independent repetitions, for two sampling strategies: standard Gaussian and  $Q_n$ ; the true integral value is shown as a dashed red line. Right: total posterior variance versus the number of evaluations for both strategies.

It is important to note that the Gaussian kernel induces a reproducing kernel Hilbert space whose norm is equivalent to that of a Sobolev space of arbitrary integer order  $\alpha \in \mathbb{N}$ . As a consequence, the variance decay reduction of Corollary 5 in this example holds for any  $\alpha$ , and thus the associated posterior variance decays faster than any polynomial. While this leads to excellent empirical performance, it may not always be suitable because it assumes the GP to have mean square derivatives of all orders, and is thus very smooth. To obtain a more flexible example, we therefore consider an alternative model based on a Matérn kernel, which induces a function space with finite smoothness.

### 5.3 Matérn Kernel

The Matérn kernel with smoothness parameter  $\alpha > 0$  is defined as

$$k_\alpha(x, x') = \sigma_f^2 \frac{2^{1-\alpha}}{\Gamma(\alpha)} \left( \frac{\sqrt{2\alpha}}{\ell} |x - x'| \right)^\alpha K_\alpha \left( \frac{\sqrt{2\alpha}}{\ell} |x - x'| \right),$$

where  $\ell > 0$  is the lengthscale,  $\sigma_f^2 > 0$  is the signal variance,  $\Gamma(\cdot)$  is the Gamma function, and  $K_\alpha(\cdot)$  denotes the modified Bessel function of the second kind [Rasmussen and Williams, 2006].

The parameter  $\alpha$  controls the smoothness of sample paths, with larger values corresponding to smoother functions. In this work, we focus on the case  $\alpha = 3/2$ , for which the kernel simplifies to the explicit form

$$k_{3/2}(x, x') = \sigma_f^2 \left( 1 + \frac{\sqrt{3}}{\ell} |x - x'| \right) \exp \left( -\frac{\sqrt{3}}{\ell} |x - x'| \right).$$

As in the Gaussian case, Bayesian quadrature requires the computation of the kernel mean  $m_{\Pi, \alpha}(x) = \int_{\mathbb{R}} k_{\alpha}(x, x') d\Pi(x')$ , where  $\Pi = \mathcal{N}(0, 1)$ . For general  $\alpha$ , this quantity does not admit a simple closed form. However, for  $\alpha = 3/2$  (and in general if  $\alpha = p + 1/2$ ,  $p \in \mathbb{N}$ ), it can be computed analytically as

$$m_{\Pi, 3/2}(x) = \sigma_f^2 \frac{e^{-x^2/2}}{\sqrt{2\pi}} \left[ T_{\ell} \left( \frac{\sqrt{3}}{\ell} - x \right) + T_{\ell} \left( \frac{\sqrt{3}}{\ell} + x \right) \right],$$

where  $T_{\ell}(\beta) = I_0(\beta) + \frac{\sqrt{3}}{\ell} I_1(\beta)$ , with  $I_0(\beta) = \sqrt{\frac{\pi}{2}} \exp\left(\frac{\beta^2}{2}\right) \operatorname{erfc}\left(\frac{\beta}{\sqrt{2}}\right)$ ,  $I_1(\beta) = 1 - \beta I_0(\beta)$  and  $\operatorname{erfc}(\cdot)$  denotes the complementary error function. Similarly, the prior variance of the integral is given by  $\operatorname{Var}_{\alpha}[\Pi(f)] = \int_{\mathbb{R}} \int_{\mathbb{R}} k_{\alpha}(x, x') d\Pi(x) d\Pi(x')$  which, for  $\alpha = 3/2$ , admits again the closed form expression

$$\operatorname{Var}_{3/2}[\Pi(f)] = \sigma_f^2 \frac{1}{\sqrt{\pi}} \left[ I_0 \left( \frac{\sqrt{3}}{\ell} \right) + \frac{\sqrt{3}}{\ell} I_1 \left( \frac{\sqrt{3}}{\ell} \right) \right],$$

where  $I_0\left(\frac{\sqrt{3}}{\ell}\right) = \sqrt{\pi} \exp\left(\frac{3}{\ell^2}\right) \operatorname{erfc}\left(\frac{\sqrt{3}}{\ell}\right)$  and  $I_1\left(\frac{\sqrt{3}}{\ell}\right) = 2 - 2\frac{\sqrt{3}}{\ell} I_0\left(\frac{\sqrt{3}}{\ell}\right)$ . These expressions enable efficient and exact computation of the Bayesian quadrature posterior in the case  $\alpha = 3/2$ .

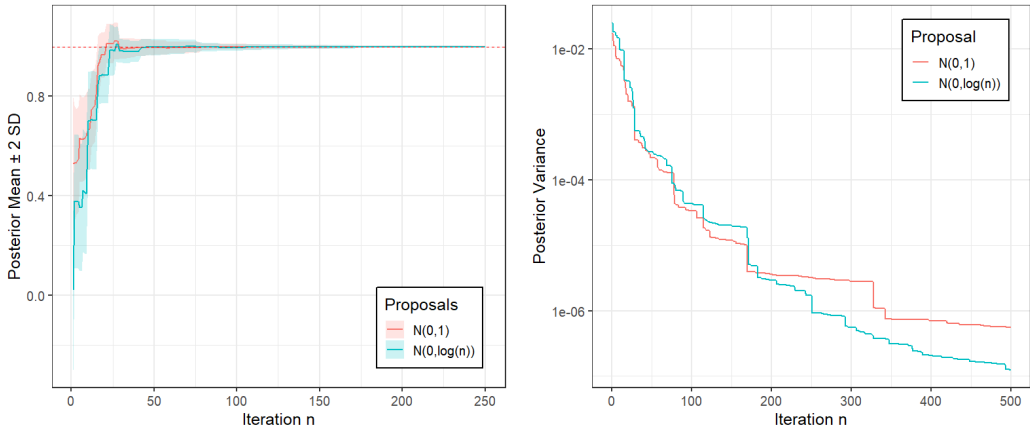


**Figure 4:** Left: posterior mean (solid lines) with  $\pm 2$  standard deviation bands over 250 sequential design iterations for two sampling strategies: standard Gaussian and  $Q_n$ ; the true integral value is shown as a dashed red line. Right: posterior variance (log scale) versus the number of evaluations for both strategies.

As in the previous experiments, the kernel hyperparameters are estimated in the same manner, but now using a Matérn kernel with smoothness parameter  $\alpha = 3/2$  instead of the RBF kernel. This yields posterior average hyperparameters  $\bar{\theta}_T = (\bar{\sigma}_{f,T}^2, \bar{\ell}_T) \approx (0.40, 0.21)$ . In contrast to the RBF case, we consider a larger number of evaluations, setting  $n = 500$  rather than 150. This choice is motivated by the slower decay of uncertainty induced by the Matérn kernel, which necessitates a longer evaluation horizon in order to clearly observe the differences between the two sampling strategies. Figure 4 compares the standard Gaussian sampling strategy with  $Q_n$ , in the same manner as Figure 2. The qualitative behavior is consistent with the RBF case: sampling from  $Q_n$  leads to a faster reduction in posterior uncertainty. After 500 evaluations, the

posterior variance is approximately  $1.24 \times 10^{-7}$  when using  $Q_n$ , compared to  $5.62 \times 10^{-7}$  under standard Gaussian sampling. Figure 5 presents results averaged over repeated experiments, following the same procedure as in Figure 3. The same trends are observed: the sampling strategy based on  $Q_n$  provides a more representative quantification of uncertainty, with larger variance at early iterations and a more rapid contraction thereafter. At the final iteration, the total posterior variance is approximately  $2.63 \times 10^{-7}$  for  $Q_n$ , compared to  $1.47 \times 10^{-6}$  for the standard Gaussian strategy.

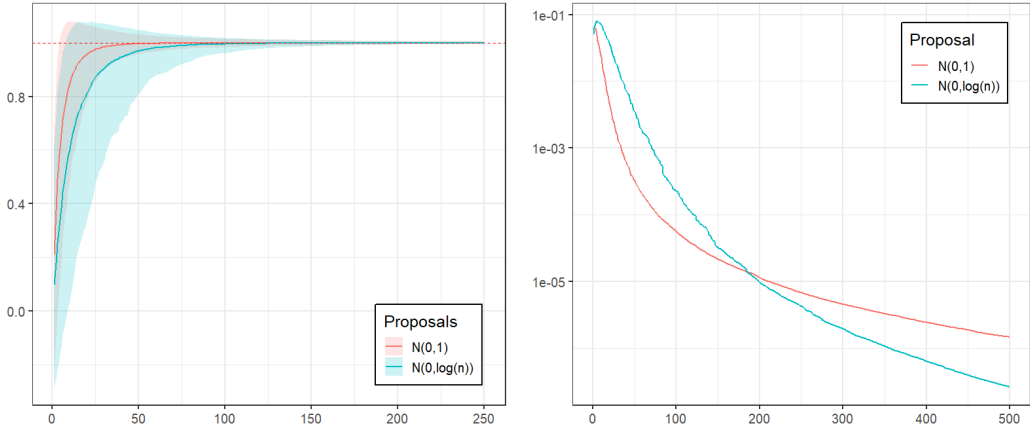


**Figure 5:** Left: average posterior mean (solid lines) with 95% uncertainty bands over sequential design iterations, computed from 1,000 independent repetitions, for two sampling strategies: standard Gaussian and  $Q_n$ ; the true integral value is shown as a dashed red line. Right: total posterior variance versus the number of evaluations for both strategies.

## 5.4 Matérn Kernel and Student- $t$ Measure

We now consider a setting where the target measure is no longer Gaussian but instead a Student- $t$  distribution with  $\nu = 5$  degrees of freedom, denote by  $\Pi$  and  $t_5$  respectively its measure and density. This choice introduces heavier tails relative to the Gaussian case and serves to illustrate the applicability of the proposed framework beyond Gaussian integration measures. Let  $f(x) = 1 + \sin(2\pi x)$ , then  $\Pi(f) = 1$ . Now define  $g(x) = f(x) \frac{t_5(x)}{t_{4.49}(x)}$ . Then, by a change of measure,

$$\int f(x) t_5(x) dx = \int g(x) t_{4.49}(x) dx,$$

where we obtain that  $g \in \mathcal{H}^\alpha(\mathbb{R}^d)$  for all  $\alpha \geq 1$ . The Gaussian process prior is equipped again with a Matérn kernel with smoothness parameter  $\alpha = 3/2$ . Unlike the case with Gaussian measure considered in the previous experiment, the kernel mean embedding  $m_{\Pi,3/2}(x)$  and the prior variance of the integral  $\text{Var}_{3/2}[\Pi(f)]$  do not admit closed-form expressions when  $\Pi = t_{4.49}$ . The prior variance is therefore approximated via Monte Carlo by drawing  $10^8$  independent samples from the  $t_{4.49}$  distribution and averaging the corresponding kernel evaluations. In contrast, the kernel mean is computed deterministically using R's `integrate()` function, which evaluates the associated one-dimensional integral of the Matérn 3/2 kernel against the  $t_8$  density to high relative tolerance. The kernel hyperparameters are estimated via the same MCMC procedure as in the preceding experiments.

The two sampling strategies under comparison are now: (i) the standard Student- $t$  distribution  $t_{4.49}$ , which coincides with the integration measure; and (ii) an inflated Student- $t$  distribution  $t_{4.49}$  scaled by  $n^{3/6.49}$ , which plays the role of  $Q_n$  from Theorem 1 adapted to the present setting. The experiment is otherwise conducted identically to the previous subsections, with  $n = 500$  sequential design evaluations.

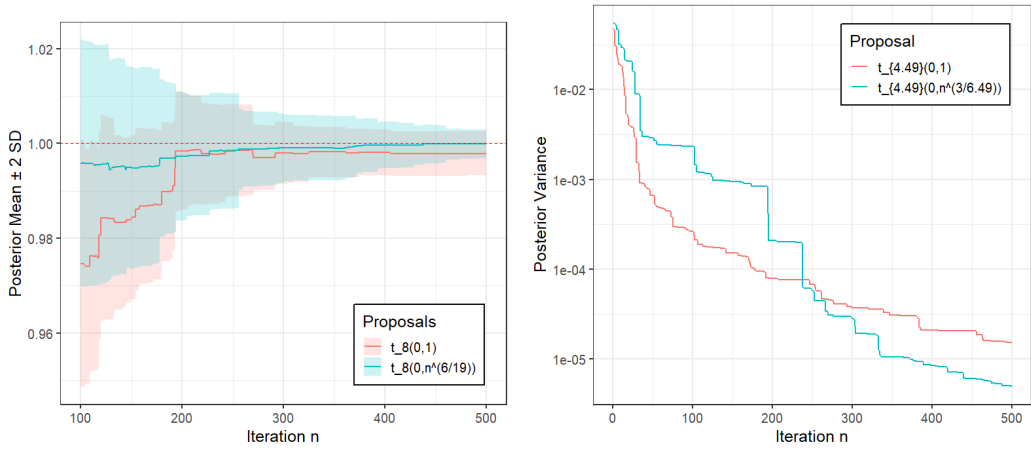


**Figure 6:** Left: posterior mean (solid lines) with  $\pm 2$  standard deviation bands over the last 400 sequential design iterations for two sampling strategies: standard  $t_{4.49}$  and inflated  $t_{4.49}$ ; the true integral value is shown as a dashed red line. Right: posterior variance (log scale) versus the number of evaluations for both strategies.

Figure 6 presents results from a single run. The posterior mean obtained under the inflated  $t_{4.49}$  strategy converges faster toward the true integral value of 1, and same for the posterior variance than under the standard  $t_{4.49}$  strategy. However, the separation between the two strategies is considerably less pronounced than in the RBF or Matérn 3/2 experiments with Gaussian measure. Figure 7 presents the results averaged over  $N = 1,000$  independent repetitions.

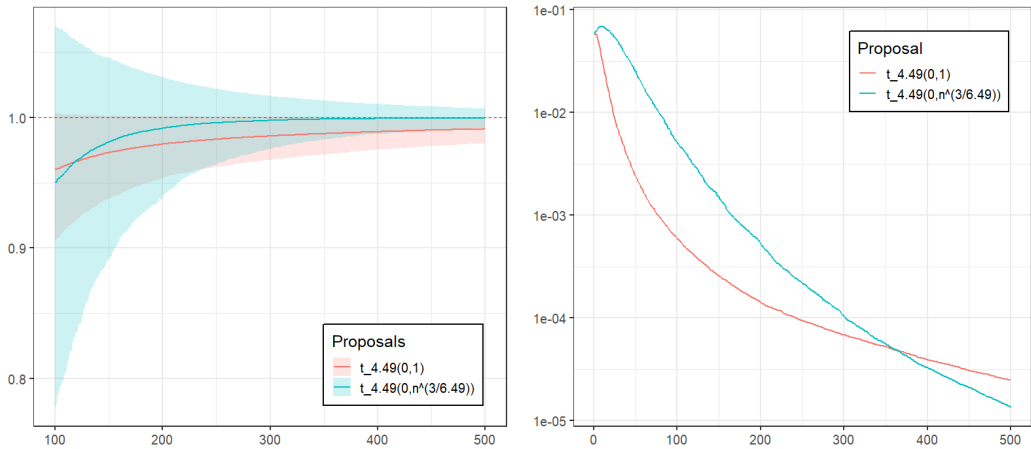


**Figure 7:** Left: average posterior mean (solid lines) with 95% uncertainty bands over sequential design iterations, computed from 1,000 independent repetitions, for two sampling strategies: standard  $t_{4.49}$  and inflated  $t_{4.49}$ ; the true integral value is shown as a dashed red line. Right: total posterior variance versus the number of evaluations for both strategies.

tions, following the same procedure as in Figures 3 and 5. The averaged results confirm the single-run findings: the inflated  $t_{4.49}$  strategy achieves a lower total posterior variance at the final iteration, and posterior mean is much closer to the true integral solution, resulting also in a slightly biased estimator when using  $t_{4.49}$ . At  $n = 500$  evaluations, the total posterior variance and the posterior mean are approximately  $1.35 \times 10^{-5}$  and 0.9996 for the inflated  $t_{4.49}$  strategy, compared to  $2.48 \times 10^{-5}$  and 0.9911 for the standard  $t_{4.49}$  strategy.

## 6 Conclusion

This paper studied randomized kernel quadrature on unbounded domains, with a focus on constructing explicit sampling distributions that achieve optimal convergence rates for worst-case integration error over Sobolev smoothness classes.

The central obstacle is that standard approaches to minimax-optimal quadrature on compact domains break down on  $\mathbb{R}^d$ : a change-of-variables reduction to  $[0, 1]^d$  destroys the smoothness of the integrand, as illustrated in Section 4.1, and naive sampling from the target measure leaves the tails of the integration measure systematically underexplored. Our solution is to work directly on  $\mathbb{R}^d$  and to inflate the sampling distribution by an  $n$ -dependent factor, chosen to balance two competing sources of error: the tail truncation bias, which penalises undersampling in the tails, and the fill-distance approximation error, which penalises insufficient coverage of the bulk.

For a Gaussian target  $\Pi = \mathcal{N}(0, I_d)$ , Theorem 1 shows that sampling from  $\mathcal{N}(0, (\alpha \log n)I_d)$  achieves the rate  $n^{-\alpha/d+\varepsilon}$ , matching the minimax-optimal rate, up to an  $\varepsilon$  factor, for integration in Sobolev spaces of smoothness  $\alpha$  in dimension  $d$  established by Novak [1988] and recovered by Briol et al. [2019] in the compact setting. For a Student- $t$  target  $\Pi = t_\nu(0, I_d)$ , Theorem 1 shows that sampling from  $t_\nu(0, n^{2\alpha/(d(\alpha+\nu+d/2))}I_d)$  achieves the rate  $n^{-\alpha(\nu+d/2)/(d(\alpha+\nu+d/2))+\varepsilon}$ , and in Theorem 3 we proved that it is the minimax. This rate reflects a genuine statistical difficulty introduced by heavy tails: it is strictly slower than the Gaussian rate, and recovers  $n^{-\alpha/d}$  only in the limit  $\nu \rightarrow \infty$ . Both results are kernel-agnostic: the optimal sampling distribution depends only on the target measure and not on the specific kernel, while in the Student- $t$  case it depends only on the Sobolev equivalence class, providing robustness to kernel misspecification. Corollary 2 shows that both rates are attained by a sequential sampling scheme, so the final sample size need not be specified in advance to maintain the rate. Proposition 4 and Corollary 5 extend the convergence guarantees to the total posterior variance, accounting simultaneously for uncertainty in the Gaussian process model and the randomness of the design points.

Several directions for future work follow naturally from the present results. A first question is whether adaptivity to the smoothness parameter  $\alpha$  is possible in the Student- $t$  case: unlike the Gaussian case, where  $\alpha$  enters the sampling variance only as a multiplicative constant and can be absorbed into the asymptotic rate, the Student- $t$  proposal depends explicitly on  $\alpha$  through the exponent of  $\Sigma_n$ . A natural direction is to further investigate the role of the proposal family: in this work, the sampling distributions achieving asymptotically optimal rates are chosen within the same parametric class as the measure of the integral (Gaussian or Student- $t$ ), with the main degree of freedom being an  $n$ -dependent inflation of the variance. While this restriction is sufficient to recover minimax rates, it may be overly conservative, and more flexible or structurally different proposal families could potentially yield improved practical performance despite having the same asymptotic guarantees. Finally, on the practical side, the sampling distributions constructed here are explicitly  $n$ -dependent, which raises the question of how to implement them efficiently in sequential settings where evaluations arrive one at a time: Corollary 2 provides a theoretical answer, but an adaptive implementation which exploits also the information of the integrand may be faster in practice, even though, as outlined in Bach [2017], [Novak, 1988, Page 17] shows that adaptive quadrature rules where points are selected sequentially with the knowledge of the function values at previous points cannot improve the worst-case guarantees. Another natural direction is to investigate how the results change when function evaluations are no longer exact, but are corrupted by noise or subject to numerical error. In this setting, both the construction of the sampling distribution and the resulting convergence rates may be affected.

The analysis presented in this work can be extended beyond the Gaussian and Student- $t$  settings. In particular, distributions with radially decaying tails can be treated using similar

arguments. In these cases, Euclidean balls maximize the measure among sets of fixed volume, which simplifies the analysis by reducing it to radially symmetric regions. Extending these results to more general measures would likely require characterizing the sets that are extremal in this sense. Moreover, the results can be extended to Gaussian kernels, or more generally to kernels inducing spaces of infinite smoothness, in which case exponentially decaying worst-case error rates can be achieved. However, the results of Proposition 4 and Corollary 5 do not directly carry over to this setting, as they would require the fill distance bound of Lemma 8 to hold with exponentially high probability, whereas the current analysis establishes this result only with polynomially high probability. Other extensions can be developed for alternative surrogate models, such as Student- $t$  processes Shah et al. [2014], Prüher et al. [2017], suggesting that the overall framework is not restricted to Gaussian process priors. Finally, although the present analysis can be extended to functions without mass decay (provided the integral is well defined) via a suitable change of measure, it may be possible to generalize the results further without such a transformation. In particular, one could aim to cover classes of functions that are locally Sobolev and bounded in  $L^\infty$ . Appendix B provides preliminary numerical evidence in this direction, together with a more detailed discussion.

## References

- M. Adachi, S. Hayakawa, M. Jørgensen, H. Oberhauser, and M. A. Osborne. Fast Bayesian Inference with Batch Bayesian Quadrature via Kernel Recombination. In *Advances in Neural Information Processing Systems (NeurIPS 2022)*, volume 35, pages 16533–16547, 2022.
- R. A. Adams. *Sobolev Spaces*. Academic Press, New York, 1975.
- F. Bach. On the equivalence between kernel quadrature rules and random feature expansions. *Journal of Machine Learning Research*, 18(21):1–38, 2017.
- A. Belhadji, R. Bardenet, and P. Chainais. Kernel quadrature with dpps. In *Advances in Neural Information Processing Systems*, 2019.
- A. Berlinet and C. Thomas-Agnan. *Reproducing kernel Hilbert spaces in probability and statistics*. Springer Science & Business Media, New York, NY, USA, 2011. ISBN 9781441973104.
- S. Boucheron, G. Lugosi, and P. Massart. *Concentration Inequalities: A Nonasymptotic Theory of Independence*. Oxford University Press, Oxford, UK, 2013.
- F. Briol, C. J. Oates, M. Girolami, and M. A. Osborne. Frank-wolfe bayesian quadrature: Probabilistic integration with theoretical guarantees. In *Advances in Neural Information Processing Systems*, volume 28, pages 1162–1170. NeurIPS, 2015.
- F.-X. Briol, C. J. Oates, J. Cockayne, W. Y. Chen, and M. Girolami. On the sampling problem for kernel quadrature. In D. Precup and Y. W. Teh, editors, *Proceedings of the 34th International Conference on Machine Learning*, volume 70 of *Proceedings of Machine Learning Research*, pages 586–595. PMLR, 06–11 Aug 2017.
- F.-X. Briol, C. J. Oates, M. Girolami, M. A. Osborne, and D. Sejdinovic. Probabilistic integration: A role in statistical computation? *Statistical Science*, 34(1):1–22, 2019. doi: 10.1214/18-STS660.
- Z. Chen, M. Naslidnyk, and F.-X. Briol. Nested expectations with kernel quadrature. In *Proceedings of the 42nd International Conference on Machine Learning*, volume 267 of *Proceedings of Machine Learning Research*, pages 8760–8793. PMLR, 2025.

- R. Durrett. *Probability: Theory and Examples*. Cambridge University Press, Cambridge, UK, 5th edition, 2019. ISBN 9781108473682.
- W. Feller. *An Introduction to Probability Theory and Its Applications, Volume II*. John Wiley & Sons, New York, NY, USA, 2nd edition, 1971. ISBN 9780471257097.
- F. L. Fernández, L. Martino, V. Elvira, D. Delgado-Gómez, and J. López-Santiago. Adaptive quadrature schemes for bayesian inference via active learning. *IEEE Access*, 8:208462–208483, 2020. doi: 10.1109/ACCESS.2020.3038333.
- M. Fisher, C. Oates, C. Powell, and A. Teckentrup. A locally adaptive bayesian cubature method. In *Proceedings of the Twenty Third International Conference on Artificial Intelligence and Statistics*, volume 108 of *Proceedings of Machine Learning Research*, pages 1265–1275. PMLR, 2020a.
- M. Fisher, C. Oates, C. Powell, and A. Teckentrup. A locally adaptive bayesian cubature method. In S. Chiappa and R. Calandra, editors, *Proceedings of the Twenty Third International Conference on Artificial Intelligence and Statistics*, volume 108 of *Proceedings of Machine Learning Research*, pages 1265–1275. PMLR, 2020b.
- T. Gunter, M. A. Osborne, R. Garnett, P. Hennig, and S. J. Roberts. Sampling for inference in probabilistic models with fast bayesian quadrature. In Z. Ghahramani, M. Welling, C. Cortes, N. D. Lawrence, and K. Q. Weinberger, editors, *Advances in Neural Information Processing Systems 27*, pages 2789–2797. Curran Associates, Inc., 2014.
- S. Hayakawa, H. Oberhauser, and T. J. Lyons. Positively weighted kernel quadrature via subsampling. In *Advances in Neural Information Processing Systems 35*, 2022.
- P. Hennig, M. A. Osborne, and M. Girolami. *Probabilistic Numerics: Computation as Machine Learning*. Cambridge University Press, 2022. doi: 10.1017/9781108671879.
- M. Kanagawa and P. Hennig. Convergence guarantees for adaptive bayesian quadrature methods. In *Advances in Neural Information Processing Systems 32*, pages 6234–6245. Curran Associates, Inc., 2019.
- M. Kanagawa, B. K. Sriperumbudur, and K. Fukumizu. Convergence analysis of deterministic kernel-based quadrature rules in misspecified settings. *Foundations of Computational Mathematics*, 20(1):155–194, 2020a.
- M. Kanagawa, B. K. Sriperumbudur, and K. Fukumizu. Convergence analysis of deterministic kernel-based quadrature rules in misspecified settings. *Foundations of Computational Mathematics*, 20:155–194, 2020b. doi: 10.1007/s10208-018-09407-7.
- T. Karvonen and S. Särkkä. Classical quadrature rules via gaussian processes. In *Proceedings of the 27th IEEE International Workshop on Machine Learning for Signal Processing (MLSP)*, pages 31–46, Tokyo, Japan, 2017. doi: 10.1109/MLSP.2017.8168195.
- T. Karvonen, M. Kanagawa, and S. Särkkä. On the positivity and magnitudes of bayesian quadrature weights. *Statistics and Computing*, 29:1317–1333, 2019. doi: 10.1007/s11222-019-09901-0.
- M. Mahsereci and T. Karvonen. Bayesian quadrature: Gaussian processes for integration. *arXiv:2602.16218*, 2026. arXiv preprint.

- P. Massart. *Concentration Inequalities and Model Selection*, volume 1896 of *Lecture Notes in Mathematics*. Springer, Berlin, Heidelberg, 2007. ISBN 978-3-540-37575-5.
- E. Novak. *Deterministic and Stochastic Error Bounds in Numerical Analysis*, volume 1349 of *Lecture Notes in Mathematics*. Springer-Verlag, Berlin, Heidelberg, 1988. ISBN 978-3-540-50368-2.
- M. A. Osborne, R. Garnett, Z. Ghahramani, D. Duvenaud, S. J. Roberts, and C. E. Rasmussen. Active learning of model evidence using bayesian quadrature. In *Advances in Neural Information Processing Systems (NeurIPS)*, volume 25, pages 46–54. Curran Associates, Inc., 2012.
- J. Prüher, F. Tronarp, T. Karvonen, S. Särkkä, and O. Straka. Student-t process quadratures for filtering of non-linear systems with heavy-tailed noise. In *20th International Conference on Information Fusion (FUSION)*, pages 875–882. IEEE, 2017.
- C. E. Rasmussen and C. K. I. Williams. *Gaussian Processes for Machine Learning*. MIT Press, Cambridge, MA, 2006.
- C. P. Robert and G. Casella. *Monte Carlo Statistical Methods*. Springer, New York, 2nd edition, 2004.
- G. O. Roberts and J. S. Rosenthal. Harris recurrence of metropolis-within-gibbs and trans-dimensional markov chains. *The Annals of Applied Probability*, 16(4):2123–2139, Nov. 2006.
- S. Särkkä, J. Hartikainen, L. Svensson, and F. Sandblom. On the relation between gaussian process quadratures and sigma-point methods. *Journal of Advances in Information Fusion*, 11(1):31–46, 2016. doi: 10.5270/JAIF11-1-204.
- A. Shah, A. G. Wilson, and Z. Ghahramani. Student-t processes as alternatives to gaussian processes. In *Proceedings of the 17th International Conference on Artificial Intelligence and Statistics (AISTATS)*, volume 33 of *Proceedings of Machine Learning Research*, pages 877–885. PMLR, 2014.
- D. Simpson, G. Riutort-Mayol, M. Binois, et al. Marginalising over stationary kernels with Bayesian quadrature. *Advances in Neural Information Processing Systems*, 2021.
- A. V. Suldin. Wiener measure and its applications to approximation methods. i. *Izvestiya Vysshikh Uchebnykh Zavedenii. Matematika*, pages 145–158, 1959. in Russian.
- E. Wagstaff, S. Hamid, and M. A. Osborne. Batch selection for parallelisation of bayesian quadrature. *arXiv preprint arXiv:1812.01553*, 2018.
- H. Wendland. *Scattered Data Approximation*. Cambridge Monographs on Applied and Computational Mathematics. Cambridge University Press, 2004.
- H. Wendland and C. Rieger. Approximate interpolation with applications to selecting smoothing parameters. *Numerische Mathematik*, 101(4):729–748, 2005. doi: 10.1007/s00211-005-0637-y.
- Z. Wu and R. Schaback. Local error estimates for radial basis function interpolation of scattered data. *IMA Journal of Numerical Analysis*, 13(1):13–27, 1993.
- G. Wynne, F.-X. Briol, and M. Girolami. Convergence guarantees for gaussian process means with misspecified likelihoods and smoothness. *Journal of Machine Learning Research*, 22(123):1–40, 2021.

# A Proofs

We first prove a concentration result. The following lemma shows that the fraction of samples lying within one Mahalanobis unit of the mean is close to its population value. In particular, with exponentially high probability, a constant fraction of the sample points lies in this central region.

**Lemma 7.** *Let  $X_1, \dots, X_n$  be i.i.d. random vectors in  $\mathbb{R}^d$ , and let  $\Sigma$  definite positive. Define the Mahalanobis norm  $\|x\|_{\Sigma^{-1}}^2 := x^\top \Sigma^{-1} x$ , and  $p := \mathbb{P}(\|X\|_{\Sigma^{-1}} \leq 1)$ . Then,*

$$\mathbb{P}\left(\#\{i : \|X_i\|_{\Sigma^{-1}} \leq 1\} \geq \frac{p}{2}n\right) \geq 1 - \exp\left(-\frac{p}{8}n\right).$$

*Proof.* Define  $Y_i := \mathbf{1}\{\|X_i\|_{\Sigma^{-1}} \leq 1\}$ ,  $i = 1, \dots, n$ , and let  $S_n := \sum_{i=1}^n Y_i$ . Since the  $X_i$  are i.i.d., the variables  $Y_i$  are i.i.d. Bernoulli with parameter  $\mathbb{P}(Y_i = 1) = p$ . Hence,  $S_n \sim \text{Binomial}(n, p)$ , with  $\mathbb{E}[S_n] = pn$ . By the multiplicative Chernoff bound [Boucheron et al., 2013], for any  $\delta \in (0, 1)$ ,

$$\mathbb{P}(S_n \leq (1 - \delta)pn) \leq \exp\left(-\frac{\delta^2}{2}pn\right).$$

Taking  $\delta = \frac{1}{2}$ , we obtain  $\mathbb{P}(S_n \leq \frac{p}{2}n) \leq \exp(-\frac{p}{8}n)$ . Taking complements yields the claim.  $\square$

We now establish how our sampling strategy controls the fill distance on the "effective domain"  $B_{R_n}$ . Intuitively, since the density  $q_n$  is radially decreasing, points are more likely near the center, and the lemma below quantifies the resulting coverage of the domain.

**Lemma 8.** *Let  $d \geq 1$ ,  $R_n > 0$  depending on  $n$  and  $B_{R_n} \subset \mathbb{R}^d$  be the ball centered in 0 with radius  $R_n$ . If  $\mathbf{x}_{1:n} = (x_1, \dots, x_n)$  are i.i.d. sampled from a distribution with an  $L$ -Lipschitz, with 0 mean and radially decreasing probability density function  $q_n$  in  $B_{R_n}$ , such that  $a_n = nq_n(R_n e) = \mathcal{O}(n^p)$  for some  $p > 0$  and any unit vector  $e \in \mathbb{R}^d$ . Then, the fill distance on  $B_{R_n}$  decays with high probability at the following rate*

$$h_{\mathbf{x}_{1:n}, B_{R_n}} = O_P\left(\left(\frac{\log n}{a_n}\right)^{1/d}\right) = O_P(n^{-p/d+\varepsilon}).$$

*Proof of Lemma 8.* Let  $B_h(x) = \{y \in \mathbb{R}^d : \|y - x\|_2 < h\}$  be the ball centered in  $x$  with radius  $h$ . Then, for any  $x \in B_{R_n}$  and  $h > 0$ , define

$$p_{h,n}(x) := \int_{B_h(x)} q_n(y) dy$$

the probability that a single sample falls in  $B_h(x)$ . Since  $q_n$  is  $L$ -Lipschitz on  $B_{R_n}$ , we have that for small  $h$

$$p_{h,n}(x) = q_n(x)|B_h(0)| + \mathcal{O}(h^{d+1}) = v_d h^d \phi_n(x) + \mathcal{O}(h^{d+1}),$$

where  $v_d = |B_1(0)|$  is the Lebesgue measure of the unit ball in  $\mathbb{R}^d$ . Let's proceed by empty-ball probabilities [Durrett, 2019], conditioning on  $x \in B_{R_n}$ , the probability that none of the points fall in  $B_h(x)$  is

$$\mathbb{P}\left(\min_{i=1, \dots, n} \|x - x_i\|_2 > h\right) = (1 - p_{h,n}(x))^n \leq \exp(-np_{h,n}(x)) \leq \exp(-v_d n h^d q_n(x)).$$

Denote by  $\mathcal{P}_{h/2}$  an  $h/2$ -net of  $B_{R_n}$ , its cardinality satisfies  $m \leq C_d(R_n/h)^d$  [Massart, 2007]. By the covering property, if the minimal distance from each point to the sample set is at most  $h/2$ , then the fill distance satisfies  $h_{\mathbf{x}_{1:n}, B_{R_n}} \leq h$ . So,

$$\mathbb{P}(h_{\mathbf{x}_{1:n}, B_{R_n}} > h) \leq \sum_{x_k \in \mathcal{P}_{h/2}} \mathbb{P}\left(\min_{i=1, \dots, n} \|x_k - x_i\|_2 > h/2\right) \leq m \exp\left(-v_d n (h/2)^d \inf_{x \in B_{R_n}} q_n(x)\right),$$

where, since  $q_n$  is radially decreasing, the minimum occurs at  $\|x\|_2 = R_n$ . Hence,

$$\mathbb{P}(h_{\mathbf{x}_{1:n}, B_{R_n}} > h) \leq C_d \frac{R_n^d}{h^d} \exp(-v_d n h^d q_n(R_n e)),$$

where  $e$  is a unit norm vector in  $\mathbb{R}^d$ . Now, observe that since  $q_n$  is radially decreasing and defined on  $\mathbb{R}^d$ , there exists  $1 \geq Z \geq 0$  such that

$$1 \geq Z = \int_{B_{R_n}} q_n(x) dx \geq q_n(R_n e) |B_{R_n}| = v_d R_n^d q_n(R_n e), \quad (1)$$

so necessarily  $R_n^d \leq 1/(v_d q_n(R_n e))$ . Thus, we obtain

$$\mathbb{P}(h_{\mathbf{x}} > h) \leq C_d \frac{1}{h^d q_n(R_n e)} \exp(-v_d n h^d q_n(R_n e))$$

and we can set the failure probability equal to  $n^{-c}$  and solve for  $h$ ,

$$C_d \frac{1}{h^d q_n(R_n e)} \exp(-v_d n h^d q_n(R_n e)) \leq n^{-c}.$$

Recall that by assumption  $a_n = n q_n(R_n e) = \mathcal{O}(n^p)$ , for some  $p > 0$ . Finally, we set  $h^d = A \log n / a_n$  which converges to zero as  $n \rightarrow \infty$ , so that the exponential term behaves like  $n^{-v_d A}$ , while the polynomial factor reduces to  $n/(A \log n)$ . Therefore, the inequality A reduces to

$$\frac{n}{\log n} n^{-v_d A} \leq n^{-c},$$

which is satisfied for any  $A > (c+1)/v_d$ .  $\square$

Observe that if  $R_n$  grows with  $n$ , then the exponent  $p$  in Lemma 8 must satisfy  $p < 1$ . Indeed, since  $q_n$  is radially decreasing, by (1) we have  $q_n(R_n e) \leq 1/(v_d R_n^d)$ . Combining this with the assumption  $a_n = n q_n(R_n e) = \mathcal{O}(n^p)$  gives

$$n q_n(R_n e) \leq \frac{n}{v_d R_n^d} = \mathcal{O}(n^p) \implies R_n \lesssim n^{(1-p)/d}.$$

Hence,  $p = 1$  corresponds to a fixed domain  $R_n = \mathcal{O}(1)$ , while  $p < 1$  occurs when  $R_n$  grows with  $n$ , and  $p > 1$  would require  $R_n$  shrinking. In particular, the domain radius must grow strictly slower than  $n^{1/d}$  in order for the fill distance to decrease. This is intuitive: in dimension  $d = 1$ , covering an interval of length  $n$  with  $n$  points results in a fill distance of order 1, which does not vanish as  $n \rightarrow \infty$ . In higher dimensions, the same principle holds: a rapidly expanding domain cannot be efficiently filled by a finite number of points without  $p < 1$ .

This lemma precisely quantifies how the interplay between sampling density and domain growth controls coverage, setting the stage for Theorem 1.

*Proof of Theorem 1.* Let  $R_n > 0$  and  $B_{R_n}$  the ball centered in zero with radius  $R_n$ , we decompose the error as

$$\begin{aligned} |\Pi(f) - \hat{\Pi}_n(f^*)| &= \left| \int_{\mathbb{R}^d} (f(x) - s_n(x)) d\Pi(x) \right| \leq \int_{\mathbb{R}^d} |f(x) - s_n(x)| d\Pi(x) \\ &= \int_{B_{R_n}} |f(x) - s_n(x)| d\Pi(x) + \int_{B_{R_n}^c} |f(x) - s_n(x)| d\Pi(x) \\ &=: \text{I} + \text{II} \end{aligned}$$

**Term II:**

$$\begin{aligned}
\Pi &\leq \left( \int_{B_{R_n}^c} |f(x) - s_n(x)|^2 dx \right)^{1/2} \left( \int_{B_{R_n}^c} \pi(x)^2 dx \right)^{1/2} \\
&\leq \|f - s_n\|_{L^2(\mathbb{R}^d)} \|\pi\|_{L^2(B_{R_n}^c)} \leq \|f - s_n\|_{\mathcal{H}^\alpha(\mathbb{R}^d)} \|\pi\|_{L^2(B_{R_n}^c)} \\
&\lesssim \|f\|_{\mathcal{H}^\alpha(\mathbb{R}^d)} \|\pi\|_{L^2(B_{R_n}^c)},
\end{aligned}$$

where the first inequality comes from the Cauchy-Schwartz and the last inequality comes from the norm equivalence of  $\mathcal{H}^\alpha$  and  $\mathcal{H}_k$  and the fact that  $\|s_n\|_{\mathcal{H}_k} \leq \|f\|_{\mathcal{H}_k}$ , since, in the noiseless case,  $s_n$  is the  $\mathcal{H}_k$ -orthogonal projection of  $f$  onto  $\text{span}\{k(x_i, \cdot)\}_{i=1}^n$  [Wendland \[2004\]](#). In particular,

$$\begin{aligned}
\|f - s_n\|_{\mathcal{H}^\alpha} &\leq \|f\|_{\mathcal{H}^\alpha} + \|s_n\|_{\mathcal{H}^\alpha} \lesssim \|f\|_{\mathcal{H}^\alpha} + \|s_n\|_{\mathcal{H}_k} \\
&\leq \|f\|_{\mathcal{H}^\alpha} + \|f\|_{\mathcal{H}_k} \lesssim \|f\|_{\mathcal{H}^\alpha} + \|f\|_{\mathcal{H}^\alpha} \lesssim \|f\|_{\mathcal{H}^\alpha}
\end{aligned}$$

We treat here separately the case in which  $\Pi$  is a standard Gaussian or a Student- $t$ .

- (i) If  $\Pi$  is the standard Gaussian measure, using classical Gaussian tail bounds obtained via integration by parts [Feller \[1971\]](#), [Durrett \[2019\]](#), we have  $\|\pi\|_{L^2(B_{R_n}^c)} \leq C_d R_n^{d-2} \exp(-R_n^2)$ , for  $R_n \geq 1$ . Choosing  $R_n = \sqrt{\alpha/d \log n}$ , we obtain the tail bound

$$\begin{aligned}
\Pi &\leq \|f\|_{\mathcal{H}^\alpha} C_1 R_n^{d-2} \exp(-R_n^2) \leq C_2 \|f\|_{\mathcal{H}^\alpha} (\alpha/d \log n)^{d/2-1} n^{-\alpha/d} \\
&\lesssim C \|f\|_{\mathcal{H}^\alpha} n^{-\alpha/d+\epsilon} = \mathcal{O}(n^{-\alpha/d+\epsilon}),
\end{aligned}$$

for some constant  $C > 0$  independent of  $n$ , for any  $\epsilon > 0$ .

- (ii) If  $\Pi$  is a Student- $t$  measure, using classical Student- $t$  tail bounds, we have  $\leq C_d R_n^{-d/2-\nu}$ . Choosing  $R_n = n^{\alpha/(d(\alpha+\nu+d/2))}$ , we obtain the tail bound

$$\Pi \leq C' \|f\|_{\mathcal{H}^\alpha} C_d n^{-\alpha\nu/(d(\alpha+\nu+d/2))} = \mathcal{O}(n^{-\alpha\nu/(d(\alpha+\nu+d/2))}).$$

**Term I:** We follow the proof of Theorem 1 in [Briol et al. \[2019\]](#), adapting it to the present increasing domain  $B_{R_n}$ , which satisfies the interior cone condition for any  $n \in \mathbb{N}$ . From a standard result in functional approximation due to [Wu and Schaback \[1993\]](#), [Wendland \[2004\]](#), see also [[Wendland and Rieger, 2005](#), Thm. 2.6], there exists  $C > 0$  independent of  $n$  and  $H_n = Q(\theta, \alpha)R_n > 0$  such that, for all  $x \in \Omega$ ,  $\mathbf{x}_{1:n} \subset \Omega$ , where  $\Omega$  being a bounded region satisfying the interior cone condition and  $h_{\mathbf{x}_{1:n}, \Omega} < H_n$ ,  $|f(x) - m_n(x)| \leq C h_{\mathbf{x}_{1:n}, \Omega}^\alpha \|f\|_{\mathcal{H}^\alpha}$ . For other kernels, alternative bounds are well-known; [[Wendland, 2004](#), Table 11.1]. From Lemma 8 we have that the fill distance decreases with high probability at the rate  $n^{-p/d+\epsilon}$ , for  $\epsilon > 0$  arbitrarily small, so for  $n$  big enough and  $p > 0$  it holds with high probability that  $h_{\mathbf{x}_{1:n}, B_{R_n}} < H_n = Q(\theta, \alpha)R_n$ . That is, there exists with high probability  $n_0 \in \mathbb{N}$  such that for any  $n \geq n_0$ ,  $h_{\mathbf{x}_{1:n}, B_{R_n}} < H_n$  and therefore

$$\begin{aligned}
\text{I} &= \int_{B_{R_n}} |f(x) - s_n(x)| d\Pi(x) \leq \Pi(B_{R_n}) \sup_{x \in B_{R_n}} |f(x) - s_n(x)| \\
&\leq C \|f\|_{\mathcal{H}^\alpha} h_{\mathbf{x}_{1:n}, B_{R_n}}^\alpha.
\end{aligned}$$

Now, by Lemma 7 we obtain that there exists  $0 < c < 1$  such that  $cn$  points among  $n$  sampled from a Gaussian or Student- $t$  distribution fall with exponentially high probability in 1 standard deviation. Moreover, observe that both the Gaussian and Student- $t$  distributions are Lipschitz, radially decreasing and centered in 0, so we can apply Lemma 8 and the only quantity to care about is  $a_n = nq_n(R_n e)$ , where  $q_n$  and  $R_n$  will depend on the Gaussian and Student- $t$  case and  $e$  is a unit vector in  $\mathbb{R}^d$ . Again, we treat separately  $\Pi$  Gaussian and Student- $t$ .

(i) If  $\Pi$  is Gaussian, from above we have  $R_n = \sqrt{\alpha/d \log n}$ , so

$$a_n = C_{\alpha,d} \frac{n}{(\log n)^{d/2}} = \mathcal{O}_P(n^{p-\varepsilon})$$

with  $p = 1$  and thus  $h_{\mathbf{x}_{1:n}, B_{R_n}} = \mathcal{O}_P(a_n^{-p/d+\varepsilon}) = \mathcal{O}_P(n^{-1/d+\varepsilon})$ . Finally, plugging it into Equation A the required bound is satisfied also in  $B_{R_n}$ .

(ii) If  $\Pi$  is Student- $t$ , from above we have  $R_n = n^{\alpha/(d(\alpha+\nu+d/2))}$ , so

$$a_n = C_{\alpha,d,\nu} \frac{n}{n^{\alpha/(d(\alpha+\nu+d/2))}} = \mathcal{O}_P(n^p)$$

with  $p = (\nu+d/2)/(d(\alpha+\nu+d/2))$  and thus  $h_{\mathbf{x}_{1:n}, B_{R_n}} = \mathcal{O}_P(a_n^{-p/d+\varepsilon}) = \mathcal{O}_P(n^{-(\nu+d/2)/(d(\alpha+\nu+d/2))+\varepsilon})$ . Finally, plugging it into Equation A the required bound is satisfied also in  $B_{R_n}$ .

This completes the proof for  $\mathcal{H}_k$  equal to  $\mathcal{H}^\alpha$ . More generally, if  $\mathcal{H}_k$  is norm equivalent to  $\mathcal{H}^\alpha$  then the result follows from the fact that  $\|\mu_n - \mu\|_{\mathcal{H}_k} \leq \lambda \|\mu_n - \mu\|_{\mathcal{H}^\alpha}$  for some  $\lambda > 0$ . Finally, using Lemma 3 from Briol et al. [2019] we get also the contraction rates result.  $\square$

*Proof of Corollary 2.* If the points are sampled sequentially from  $Q_n$  being respectively Gaussian or Student- $t$  distributions centered at zero with covariance matrices  $\Sigma_i \asymp s(i) I_d$  for  $i = 1, \dots, n$ , we obtain the same rates. The only difference in the proof consists of the computation of  $\mathbb{P}(\min_{i=1, \dots, n} \|x - x_i\|_2 > h)$ . In the sequential setting we get

$$\mathbb{P}\left(\min_{i=1, \dots, n} \|x - x_i\|_2 > h\right) = \prod_{i=1}^n (1 - p_{h,i}(x)) \leq \exp\left\{-\sum_{i=1}^n p_{h,i}(x)\right\},$$

where

$$p_{h,i}(x) = \int_{B_h(x)} q_i(y) dy.$$

Since  $q_i$  is centered in 0,  $L$ -Lipschitz and radially decreasing, proceeding as in Lemma 8, we obtain  $\exp(-\sum_{i=1}^n p_{h,i}(x)) \leq \exp(-2\nu_d h^d \sum_{i=1}^n q_i(x)) \leq \exp(-2\nu_d h^d \sum_{i=1}^n q_i(R_n e))$ . Thus, it remains to show  $\sum_{i=1}^n q_i(R_n e) \asymp n q_n(R_n e)$ .

**Gaussian case.** If  $s(i) \asymp \log i$ , with  $R_n^2 = \log n$ . Then  $q_i(R_n e) = (2\pi \log i)^{-d/2} \exp\left\{-\frac{R_n^2}{2 \log i}\right\}$ . Since

$$\frac{R_n^2}{2 \log i} = \frac{\log n}{2 \log i} = \frac{\log n}{\log i} \cdot \frac{1}{2},$$

let  $i_* = n^\theta$ , with  $0 < \theta < 1$ . For  $i \geq i_*$ , we have  $\log i \geq \theta \log n$ , and therefore  $\frac{R_n^2}{2 \log i} \leq \frac{1}{2\theta}$ . Thus

$$q_i(R_n e) \geq (2\pi \theta \log n)^{-d/2} \exp\left\{-\frac{1}{2\theta}\right\} \asymp q_n(R_n e).$$

Moreover, the number of such indices satisfies  $n - i_* = n(1 - n^{\theta-1}) \asymp n$ , and therefore  $\sum_{i=1}^n q_i(R_n e) \asymp n q_n(R_n e)$ , where  $n q_n(R_n e)$  is controlled in Theorem 1

**Student- $t$  case.** If  $s(i) \asymp i^{2\alpha/(d(\alpha+\nu+d/2))}$ , with  $R_n^2 = n^{2\alpha/(d(\alpha+\nu+d/2))}$ . Then

$$q_i(R_n e) = c_{\nu,d} s(i)^{-d/2} \left(1 + \frac{R_n^2}{\nu s(i)}\right)^{-(\nu+d)/2}.$$

Since

$$\frac{R_n^2}{\nu s(i)} = \frac{n^{2\alpha/(d(\alpha+\nu+d/2))}}{\nu i^{2\alpha/(d(\alpha+\nu+d/2))}} = \frac{1}{\nu} \left(\frac{n}{i}\right)^{2\alpha/(d(\alpha+\nu+d/2))},$$

let  $i_* = \theta n$ , with  $0 < \theta < 1$ . For  $i \geq i_*$ , we have  $\left(\frac{n}{i}\right)^{2\alpha/(d(\alpha+\nu+d/2))} \leq \theta^{-2\alpha/(d(\alpha+\nu+d/2))}$ , and therefore  $1 + \frac{R_n^2}{\nu s(i)} \leq 1 + \frac{1}{\nu} \theta^{-2\alpha/(d(\alpha+\nu+d/2))}$ . Hence,

$$\left(1 + \frac{R_n^2}{\nu s(i)}\right)^{-(\nu+d)/2} \geq \left(1 + \frac{1}{\nu} \theta^{-2\alpha/(d(\alpha+\nu+d/2))}\right)^{-(\nu+d)/2}.$$

Moreover, since  $s(i) \asymp i^{2\alpha/(d(\alpha+\nu+d/2))}$ , for  $i \geq i_*$  we have  $s(i) \leq s(n)$ , and  $s(i) \geq s(\theta n) \asymp \theta^{2\alpha/(d(\alpha+\nu+d/2))} s(n)$ , so that  $s(i)^{-d/2} \geq s(n)^{-d/2}$ . Combining the bounds, we obtain for all  $i \geq i_*$ ,

$$q_i(R_n e) \geq c_{\nu,d} s(n)^{-d/2} \left(1 + \frac{1}{\nu} \theta^{-2\alpha/(d(\alpha+\nu+d/2))}\right)^{-(\nu+d)/2} \asymp q_n(R_n e).$$

Finally, the number of such indices satisfies  $n - i_* = (1 - \theta)n \asymp n$ , and therefore

$$\sum_{i=1}^n q_i(R_n e) \asymp n q_n(R_n e),$$

where  $n q_n(R_n e)$  is controlled in Theorem 1.  $\square$

**Lemma 9.** Let  $\alpha > d/2$ ,  $\nu > 0$ ,  $R_n \geq 1$  and let  $p_\nu : \mathbb{R}^d \rightarrow (0, \infty)$  satisfying  $c_1(1 + \|x\|_2^2)^{-(\nu+d)/2} \leq p_\nu(x) \leq c_2(1 + \|x\|_2^2)^{-(\nu+d)/2}$  for some constants  $c_1, c_2 > 0$ . Then, there exists a constant  $c = c(\alpha, d, \nu, c_1, c_2) > 0$  such that

$$\sup_{\|f\|_{\mathcal{H}^\alpha(\mathbb{R}^d)} \leq 1} \left| \int_{B_{R_n}^c} f(x) p_\nu(x) dx \right| \geq c R_n^{-\nu-d/2}.$$

*Proof of Lemma 9.* Fix  $\psi \in C_c^\infty(B(0, 2))$  such that  $0 \leq \psi(x) \leq 1$  for any  $x \in \mathbb{R}^d$ ,  $\psi(x) = 1$  for  $\|x\|_2 \leq 1$ ,  $\text{supp}(\psi) \subset B(0, 2)$  and  $\|\psi\|_{\mathcal{H}^\alpha} = 1$ . Such  $\psi$  exists by standard mollifier constructions Adams [1975]. Let  $y_{R_n} \in \{\|x\|_2 > 2R_n\}$  such that  $B(y, R_n) \cap B_{R_n} = \emptyset$ . Define the scaled bump  $\phi_{R_n}(x) = \psi((x - y_{R_n})/R_n)$ , then  $\text{supp}(\psi) \subset B(y_{R_n}, 2R_n) \subset \{\|x\|_2 > 2R_n\}$ ,  $\phi_{R_n} = 1$  on  $B(y_{R_n}, R_n)$  and in particular  $\phi_{R_n}(x) = 0$  on  $B_{R_n}$  (by construction of  $y_{R_n}$ ). Let's compute the Sobolev norm: translation by  $y_{R_n}$  does not change the  $\mathcal{H}^\alpha$  norm, so only the dilation matters. For the standard inhomogeneous Sobolev norm,  $\|f\|_{\mathcal{H}^\alpha(\mathbb{R}^d)}^2 = \int_{\mathbb{R}^d} (1 + \|\xi\|_2^2)^\alpha |\widehat{f}(\xi)|^2 d\xi$ , a change of variables gives  $\widehat{\phi_{R_n}}(\xi) = R_n^d e^{-iy_{R_n} \cdot \xi} \widehat{\psi}(R_n \xi)$ . Hence

$$\|\phi_{R_n}\|_{\mathcal{H}^\alpha}^2 = R_n^d \int_{\mathbb{R}^d} \left(1 + \frac{\|\eta\|_2^2}{R_n^2}\right)^\alpha |\widehat{\psi}(\eta)|^2 d\eta,$$

after the substitution  $\eta = R_n \xi$ . This implies the standard estimate

$$\|\phi_{R_n}\|_{\mathcal{H}^\alpha} = C_\alpha R_n^{d/2} \max(1, R_n^{-\alpha}) \|\psi\|_{\mathcal{H}^\alpha} = C_\alpha R_n^{d/2}$$

for  $R \geq 1$ . We normalize and get  $f_{R_n}(x) = c R_n^{-d/2} \phi_{R_n}(x)$  and  $\|f_{R_n}\|_{\mathcal{H}^\alpha} = 1$ . On  $B(y_{R_n}, R_n)$  we have  $f_{R_n}(x) = c R_n^{-d/2}$ . By the tail assumption on  $p_\nu$ , we get

$$\int_{B_{R_n}^c} f_{R_n}(x) p(x) dx \geq c \int_{B(y_{R_n}, R_n)} R_n^{-d/2} p(x) dx \geq c'_1 R_n^{-(\nu+d)-d/2} \omega_d R_n^d = c_3 R_n^{-\nu-d/2}.$$

$\square$

*Proof of Theorem 3.* Let's first denote by  $\mathcal{F}_n^{(\text{in})} = \{f \in \mathcal{H}^\alpha(\mathbb{R}^d) : \|f\|_{\mathcal{H}^\alpha} \leq 1, \text{supp}(f) \subset B_{R_n}\}$  and  $\mathcal{F}_n^{(\text{out})} = \{f \in \mathcal{H}^\alpha(\mathbb{R}^d) : \|f\|_{\mathcal{H}^\alpha} \leq 1, \text{supp}(f) \subset B_{R_n}^c\}$ . Moreover, let  $R_n = \max_i \|x_i\|_2 + 1$  so that  $x_i \in B_{R_n}$  for all  $i = 1, \dots, n$ . Formally,

$$\mathcal{E}_n = \inf_{\mathcal{Q}_n} \sup_{\|f\|_{\mathcal{H}^\alpha} \leq 1} \mathcal{E}(Q_n, f) \geq \inf_{\mathcal{Q}_n} \max \left( \sup_{f \in \mathcal{F}_n^{(\text{in})}} \mathcal{E}(Q_n, f), \sup_{f \in \mathcal{F}_n^{(\text{out})}} \mathcal{E}(Q_n, f) \right),$$

where, for  $f \in \mathcal{F}_n^{(\text{in})}$ ,  $\mathcal{E}(Q_n, f) = \left| \int_{B_{R_n}} f(x) p_\nu(x) dx - \sum_{i=1}^n w_i f(x_i) \right|$  and for  $f \in \mathcal{F}_n^{(\text{out})}$ ,  $\mathcal{E}(Q_n, f) = \left| \int_{B_{R_n}^c} f(x) p_\nu(x) dx \right|$ . We bound the first term from below using the fill distance  $h_{\mathbf{x}_{1:n}, B_{R_n}}$ . By the standard scattered-data lower bound [Wendland, 2004, Novak, 1988, page 37] for any  $n$  points  $\mathbf{x}_{1:n} \subset B_{R_n}$  there exists  $g \in H^\alpha(B_R)$  with  $\|g\|_{H^\alpha} \leq 1$  such that

$$\left| \int_{B_{R_n}} g(x) p_\nu(x) dx - \sum_{i=1}^n w_i f(x_i) \right| \geq c h_{\mathbf{x}_{1:n}, B_{R_n}}^\alpha$$

for some constant  $c > 0$  independent of  $n$  and  $R$ . We now bound  $h_{\mathbf{x}_{1:n}, B_{R_n}}$  from below. Since by optimal filling criteria on  $[0, 1]^d$ , the fill distance scales at most like  $h_{\mathbf{x}_{1:n}, [0, 1]^d} \geq n^{-1/d}$  Wendland [2004], by mapping  $[0, 1]^d$  to  $B_{R_n}$ , we get

$$h_{\mathbf{x}_{1:n}, B_{R_n}} \geq c \left( \frac{R_n^d}{n} \right)^{1/d} = c R_n n^{-1/d},$$

which gives, for  $f \in \mathcal{F}_n^{(\text{in})}$ ,  $\mathcal{E}(Q_n, f) \geq c R_n^\alpha n^{-\alpha/d}$ . Moreover, Lemma 9 gives that if  $f \in \mathcal{F}_n^{(\text{out})}$ ,  $\mathcal{E}(Q_n, f) \geq c R_n^{-\nu-d/2}$ . Thus,

$$\begin{aligned} \mathcal{E}_n &\geq C \inf_{\mathcal{Q}_n} \max(R_n^\alpha n^{-\alpha/d}, R_n^{-\nu-d/2}) = C \inf_{R_n > 0} \inf_{\mathcal{Q}_n(R_n)} \max(R_n^\alpha n^{-\alpha/d}, R_n^{-\nu-d/2}) \\ &= C \inf_{R_n > 0} \max(R_n^\alpha n^{-\alpha/d}, R_n^{-\nu-d/2}), \end{aligned}$$

where we denoted by  $\mathcal{Q}_n(R_n)$  the class of quadrature rules with points distant at most  $R_n$  from the origin. Finally, by taking  $R_n$  which minimizes this maximum, i.e.  $R_n = n^{\frac{\alpha}{d(\alpha+\nu+d/2)}}$ , we obtain  $\mathcal{E}_n = n^{-\frac{\alpha(\nu+d/2)}{d(\alpha+\nu+d/2)}}$ .  $\square$

*Proof of Proposition 4.* Let us first assume that  $f \in \mathcal{H}_k$ . To prove the proposition it is sufficient to show that the variance with respect to  $\mathbf{x}_{1:n}$  of the posterior mean  $\text{Var}_{\mathbf{x}_{1:n}} [\mathbb{E}_{f^*} [\Pi(f^*) \mid \mathbf{x}_{1:n}]]$  is bounded by the RKHS norm of  $f$ ,  $\|f\|_{\mathcal{H}_k}$ . Let  $\mu_\Pi(x) := \int_{\mathcal{X}} k(x, y) d\Pi(y) \in \mathcal{H}_k$  be the kernel mean and  $\phi_{\mathbf{x}_{1:n}}(x) := \sum_{i=1}^n w_i(\mathbf{x}_{1:n}) k(x_i, x) \in \mathcal{H}_k$ . Then, we can write  $\mathbb{E}_{f^*} [\Pi(f^*) \mid \mathbf{x}_{1:n}] = \langle f, \phi_{\mathbf{x}_{1:n}} \rangle_{\mathcal{H}_k}$  Mahsereci and Karvonen [2026]. Therefore the following holds,

$$\begin{aligned} \text{Var}_{\mathbf{x}_{1:n}} [\mathbb{E}_{f^*} [\Pi(f^*) \mid \mathbf{x}_{1:n}]] &= \text{Var}_{\mathbf{x}_{1:n}} [\langle f, \phi_{\mathbf{x}_{1:n}} \rangle_{\mathcal{H}_k}] = \text{Var}_{\mathbf{x}_{1:n}} [\langle f, \mu_\Pi - \varepsilon_{\mathbf{x}_{1:n}} \rangle_{\mathcal{H}_k}] \\ &= \text{Var}_{\mathbf{x}_{1:n}} [\langle f, \varepsilon_{\mathbf{x}_{1:n}} \rangle_{\mathcal{H}_k}] \leq \mathbb{E}_{\mathbf{x}_{1:n}} [\langle f, \varepsilon_{\mathbf{x}_{1:n}} \rangle_{\mathcal{H}_k}^2] \\ &\leq \|f\|_{\mathcal{H}_k}^2 \mathbb{E}_{\mathbf{x}_{1:n}} [\text{Var}_{f^*} [\Pi(f^*) \mid \mathbf{x}_{1:n}]], \end{aligned}$$

where  $\varepsilon_{\mathbf{x}_{1:n}} := \mu_\Pi - \phi_{\mathbf{x}_{1:n}} \in \mathcal{H}_k$  and for the last inequality see [Mahsereci and Karvonen, 2026, Proposition 2.6]. Moreover, if  $\mathcal{H}_k$  is norm equivalent to  $\mathcal{H}^\alpha$  then there exists  $\lambda > 0$  such that  $\|f\|_{\mathcal{H}_k} \leq \lambda \|f\|_{\mathcal{H}^\alpha}$ . Finally,

$$\begin{aligned} \text{Var} \left[ \Pi(f^*) \mid \mathbf{x}_{1:n} \stackrel{\text{i.i.d.}}{\sim} \mathcal{Q}_n \right] &= \mathbb{E}_{\mathbf{x}_{1:n}} [\text{Var}_{f^*} [\Pi(f^*) \mid \mathbf{x}_{1:n}]] + \text{Var}_{\mathbf{x}_{1:n}} [\mathbb{E}_{f^*} [\Pi(f^*) \mid \mathbf{x}_{1:n}]] \\ &\leq \mathbb{E}_{\mathbf{x}_{1:n}} [\text{Var}_{f^*} [\Pi(f^*) \mid \mathbf{x}_{1:n}]] + \|f\|_{\mathcal{H}_k}^2 \mathbb{E}_{\mathbf{x}_{1:n}} [\text{Var}_{f^*} [\Pi(f^*) \mid \mathbf{x}_{1:n}]] \\ &\leq (1 + \lambda^2 \|f\|_{\mathcal{H}^\alpha}^2) \mathbb{E}_{\mathbf{x}_{1:n}} [\text{Var}_{f^*} [\Pi(f^*) \mid \mathbf{x}_{1:n}]] \\ &\leq C(1 + \|f\|_{\mathcal{H}^\alpha}^2) \mathbb{E}_{\mathbf{x}_{1:n}} [\text{Var}_{f^*} [\Pi(f^*) \mid \mathbf{x}_{1:n}]]. \end{aligned}$$

$\square$

*Proof of Corollary 5.* By assumption,  $f \in \mathcal{H}^\alpha$ , with  $\mathcal{H}^\alpha$  norm-equivalent to the RKHS  $\mathcal{H}_k$ , so  $\|f\|_{\mathcal{H}^\alpha}^2 < \infty$ . Thus, by Proposition 4, it is enough to prove that  $\mathbb{E}_{\mathbf{x}_{1:n}} [\text{Var}_{f^*} [\Pi(f^*) \mid \mathbf{x}_{1:n}]] = \mathcal{O}(n^{-p})$ , where  $p$  depends on the measure of the integral according to Theorem 1. By Theorem

1,  $\text{Var}_{f^*} [\Pi(f^*) \mid \mathbf{x}_{1:n}] = \mathcal{O}_P(n^{-p})$  and for simplicity we denote  $v_n = \text{Var}_{f^*} [\Pi(f^*) \mid \mathbf{x}_{1:n}]$  and  $v_0$  the prior variance, where we observe that  $v_0 \geq v_n$  for any  $n \geq 1$ . Then,

$$\begin{aligned} \mathbb{E}_{\mathbf{x}} [v_n] &= \mathbb{E}_{\mathbf{x}} [v_n 1_{\{v_n \leq Cn^{-p}\}}] + \mathbb{E}_{\mathbf{x}} [v_n 1_{\{v_n > Cn^{-p}\}}] \\ &\leq Cn^{-p} + v_0 \mathbb{E}_{\mathbf{x}} [1_{\{v_n > Cn^{-p}\}}] \\ &\leq Cn^{-p} + v_0 n^{-c}, \end{aligned}$$

where the last inequality holds since the probability that  $v_n = O(n^{-p})$  is equal to  $1 - n^{-c}$ , for any  $c > 0$ . Finally, taking  $c > p$  and  $p$  according to Theorem 1 gives the thesis.  $\square$

*Proof of Proposition 6.* The posterior  $\pi$  is strictly positive and continuous on  $(0, \infty)^2$ . The  $\sigma_f^2$  update is an exact draw from its full conditional, which has a Lebesgue density on  $(0, \infty)$ ; hence  $\mathbb{P}(\sigma_{t+1}^2 = \sigma_t^2) = 0$  and the  $\sigma_f^2$  coordinate is updated at every iteration almost surely. For the  $\ell$  update, the Metropolis–Hastings kernel has proposal density  $q(\ell, \ell') > 0$  on  $(0, \infty)^2$  and target density  $\pi(\ell \mid \sigma^2, \mathbf{f}_{1:n}) > 0$  for all  $\ell > 0$ . Hence every proposal is generated with positive probability and accepted with positive probability, implying that the MH kernel is Lebesgue-irreducible.

Consequently, from any initial state  $\theta_0$ , with probability 1 the chain updates the  $\sigma_f^2$  coordinate at every iteration and makes at least one accepted move in the  $\ell$  coordinate in finite time. Hence both component kernels satisfy the assumptions of Theorem 12 in Roberts and Rosenthal [2006], implying the joint chain is Harris recurrent. Aperiodicity follows from the positive probability of MH rejection, which induces self-transitions. Therefore the chain is aperiodic, Harris recurrent, and hence ergodic.  $\square$

## B Beyond Mass-Decaying Integrands

The analysis developed in the main text relies on assumptions ensuring sufficient mass decay of the integrand at infinity. In particular, these conditions guarantee that the target function belongs to the appropriate weighted Sobolev spaces, which in turn control the integration error. We conjecture that these assumptions can be relaxed. Specifically, it is natural to expect that similar results hold for broader classes of functions that are only locally Sobolev and bounded in  $L^\infty(\mathbb{R}^d)$ , without requiring any mass decay at infinity. A possible formal setting is to consider functions  $f$  such that

$$f \in \mathcal{H}_{\text{loc}}^\alpha(\mathbb{R}^d) \cap L^\infty(\mathbb{R}^d),$$

where local Sobolev means that the functions are Sobolev in any compact  $K \subset \mathbb{R}^d$ .

Extending the theoretical guarantees to this setting would likely require controlling the tail error using the  $L^\infty$ -norm, specifically the one of the Gaussian Process posterior mean  $s_n$ . In particular, one should expect a deterioration in the convergence rates: the dimension-dependent factor appearing in the main results (e.g., the  $d/2$  term) is unlikely to be preserved under such weaker assumptions.

To provide preliminary evidence, we report a simple numerical experiment in Figure 8. We consider the function  $f(x) = 1 + \sin(2\pi x)$ , which is bounded and smooth but does not exhibit decay at infinity. The goal is to approximate its integral with respect to a standard Gaussian measure on  $\mathbb{R}$ . We apply kernel-based quadrature methods using both a Gaussian kernel and a Matérn kernel with smoothness parameter  $3/2$ , mimicking the experiments in Section 5. Despite the lack of decay in the integrand, the empirical results indicate similar behavior as the mass decaying case.

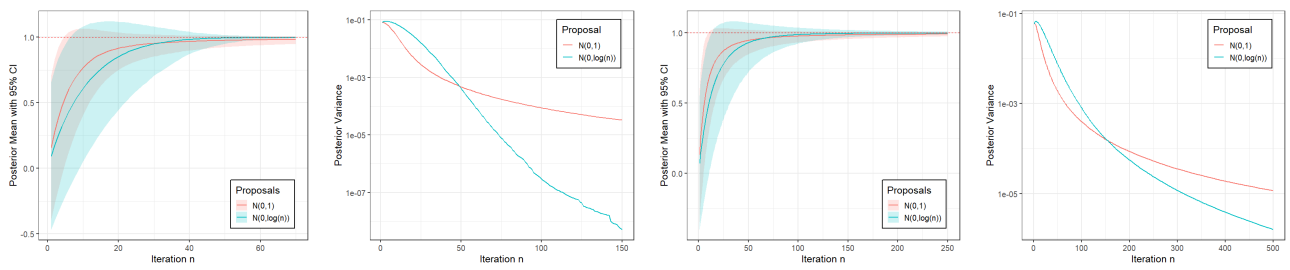


**Figure 8:** Posterior mean with 95% credible intervals and posterior variance across iterations for Gaussian and Matérn 3/2 kernels.